Automated Weather Observation Recorder

Simo Alaranta

School of Electrical Engineering

Thesis submitted for examination for the degree of Master of Science in Technology.

Espoo 4.3.2016

Thesis supervisor:

Prof. Raimo Sepponen

Thesis advisor:

M.Sc. (Tech.) Jyrki Ojanperä

Aalto University
School of Electrical Engineering

AALTO UNIVERSITY
SCHOOL OF ELECTRICAL ENGINEERING

ABSTRACT OF THE
MASTER'S THESIS

Author: Simo Alaranta

Title: Automated Weather Observation Recorder

Date: 4.3.2016 Language: English Number of pages: 6+83

Department of Electrical Engineering and Automation
Professorship: Electronics and Applications Code: S-66

Supervisor: Prof. Raimo Sepponen
Advisor: M.Sc.(Tech.) Jyrki Ojanperä

Many fields, including aeronautics and transportation, require accurate real-time weather data for predicting hazardous conditions. These fields utilize present weather information, since precipitation and reduced visibility affect their operational safety. Due to variation in the severity of the conditions arising from different precipitation types, it is vital to reliably identify the type of precipitation.

Automatic systems have increasingly been used to classify precipitations, partially replacing human observers. Although current automatic systems are able to reliably classify some precipitation types, not all precipitation types can be distinguished. For evaluation of the current automatic systems, accurate weather data is vital. In order to achieve reliable evaluation results, measurements should be compared to weather observations performed by trained observers. However, observers are required to be present during the whole evaluation period.

The goal of this thesis is to develop an automated weather observation recorder (AWORe) for recording weather conditions. AWORe utilizes two network cameras, a high-speed camera, a microphone and numerous weather instruments. AWORe enables human observers to make reliable weather observations without requiring that observers be continuously present during evaluation of weather instruments. AWORe software is developed using LabVIEW (National Instruments). In addition, a web user interface is designed, which allows users to submit weather observations as well as monitor real-time and past weather conditions.

Keywords: Automatic classification of precipitation types, system development

AALTO-YLIOPISTO
SÄHKÖTEKNIIKAN KORKEAKOULU

DIPLOMITYÖN
TIIVISTELMÄ

Tekijä: Simo Alaranta

Työn nimi: Automaattinen säähavaintojen tallennusjärjestelmä

Päivämäärä: 4.3.2016 Kieli: Englanti Sivumäärä: 6+83

Sähkötekniikan ja automaation laitos
Professuuri: Elektroniikka ja sovellukset Koodi: S-66

Työn valvoja: Prof. Raimo Sepponen
Työn ohjaaja: DI Jyrki Ojanperä

Monet alat tarvitsevat reaaliaikaista säätietoa eri tarkoituksiin. Säätietoa käytetään esimerkiksi ilmailussa turvallisten lento-olosuhteiden varmistamiseen. Sadetyypit tulee tunnistaa luotettavasti, sillä jotkut sadetyypit aiheuttavat enemmän vaaraa kuin toiset. Erityisesti jäätävät ja jäiset sateet ovat haitallisia ilmailulle sekä tieliikenteelle.

Sadetyyppien tunnistamisessa käytetään yhä enemmän automaattisia järjestelmiä. Automaattisilla järjestelmillä pystytään tunnistamaan osa sadetyypeistä luotettavasti, mutta kuitenkaan kaikkia sadetyyppejä ei nykyään pystytä tunnistamaan luotettavasti tai ollenkaan. Järjestelmien suorituskyvyn arvioimisessa tarvitaan tarkkaa tietoa vallitsevista sääolosuhteista, jotta mittaustuloksia voidaan arvioida luotettavasti. Koulutetut havainnoitsijat ovat tyypillisesti tehneet säähavainnot, joihin mittaustuloksia on voitu verrata luotettavasti. Tämä kuitenkin vaatii havainnoitsijan jatkuvaa läsnäoloa.

Tässä diplomityössä kehitettiin ja toteutettiin automaattinen säähavaintojen tallennusjärjestelmä (AWORe), joka hyödyntää kahta IP-kameraa, suurnopeuskameraa, mikrofonia sekä useita sääantureita. Järjestelmän tarkoituksena on mahdollistaa luotettavien säähavaintojen tekeminen jälkikäteen audiovisuaalisen materiaalin sekä päivittäisen raportin avulla, jolloin havainnoitsijan ei tarvitse olla jatkuvasti paikalla. Järjestelmän ohjelmisto toteutettiin National Instrumentsin LabVIEW-ohjelmalla. Ohjelmiston lisäksi järjestelmään suunniteltiin web-käyttöliittymä, jolla käyttäjät pystyvät lisäämään säähavaintoja järjestelmään sekä seuraamaan päivittäisiä säätapahtumia.

Avainsanat: Automaattinen sadetyyppien tunnistaminen, järjestelmäsuunnittelu

Preface

This thesis was carried out for R&D department of Vaisala Oyj. First, I want to thank my supervisor professor Raimo Sepponen and my advisor Jyrki Ojanperä (Engineering Manager at Vaisala Oyj) for their guidance during this writing process. Special thanks to Jarmo Räisänen (R&D Manager at Vaisala Oyj) for his professional guidance throughout the thesis. I would also like to thank individually everyone from Vaisala Oyj who shared their visions or other ways contributed to implementation of AWORe.

Espoo, 4.3.2016

Simo Alaranta

Contents

Abbreviations

AOI	Area of Interest
ASOS	Automatic Surface Observing System
AVI	Audio Video Interleave
AWORe	Automatic Weather Observation Recorder
AWOS	Automatic Weather Observing System
CoC	Circle of Confusion
CSI	Critical Success Index
DoF	Depth of Field
EV	Exposure Value
FAR	False Alarm Ratio
FOV	Field of View
FPGA	Field Programmable Gate Array
GUI	Graphical User Interface
HSC	High-speed camera
HSS	Heidke Skill Score
ICAO	International Civil Aviation Organization
LEDWI	Light Emitting Diode Weather Identifier
LV	LabVIEW
MOR	Meteorological Optical Range
NAS	Network Storage Array
NWS	National Weather Service
POD	Probability of Detection
PWS	Present Weather Sensor
RAID	Redundant Array of Independent Disks
RVR	Runway Visual Range
VI	Virtual Instrument
Web UI	Web User Interface
WMO	World Meteorological Organization

1 Introduction

Many fields, including aeronautics and transportation, require accurate real-time weather data for predicting hazardous conditions. Although trained observers typically perform weather observations, utilization of automatic weather observation systems (AWOS) has increased in recent decades. Since the reliability and measurement accuracy of AWOSs have developed over time, AWOSs have increasingly replaced human observers.

AWOSs used in airports and roadways typically utilize present weather sensors (PWS) to automatically measure precipitation intensity and accumulation as well as to classify precipitation type and determine the character of precipitations. The reliable evaluation of PWSs requires more accurate weather data than PWSs are able to provide. Therefore, human performed weather observations are currently used as a reference in PWS evaluation [1]. When a PWS is under evaluation trained observers must work over the whole evaluation period, demanding considerable resources. Moreover, human observations are subjective and may therefore lead to ambiguous results, as the weather conditions occurring at the time of a certain observation cannot be confirmed afterwards. These ambiguous results increase the uncertainty of sensor evaluation.

An alternative approach for PWS evaluation would use cameras and microphone to continuously record occurring weather conditions [2]. In addition, various weather instruments could be used to measure basic weather parameters, including temperature and relative humidity. Such an approach would allow the display of past weather conditions and later verification of the current weather conditions. Thus, no trained observers would be required during the whole evaluation period. Another advantage of this method is that the recordings and weather data could be analyzed by a group of observers, thus enabling the likelihood of more precise results.

The goal of this thesis was to develop and implement an automatic weather observation recorder (AWORe) for continuously recording weather conditions occurring at a test field. The purpose of AWORe is to allow human observers to determine the precipitation occurring at any given time without requiring human observers to be continuously present. This thesis was carried out for Vaisala Oyj, a Finnish company that develops as well as manufactures instruments and systems for environmental and industrial measurements.

AWORe performs weather recording using two network cameras, a microphone, a high-speed camera (HSC) and numerous weather instruments. The AWORe software was developed using LabVIEW (LV). In addition, a web user interface (web UI) was designed, allowing users to submit weather observations as well as monitor real-time and past weather conditions. The web UI was designed using mainly HTML5.

The gathered data enables human observers to make reliable weather observations without requiring observers to be continuously present during evaluation of PWSs. Since observers are not required to be present during the evaluation, long-term evaluations of PWSs can be performed using less resources than those currently used.

This thesis is structured as follows: Chapter 2 reviews precipitation as well as introduces currently used automatic precipitation observation methods and describes performance evaluation methods of PWSs. In addition, video recording of hydrometeors is discussed in Chapter 2. Chapter 3 presents the development and implementation process of AWORe. Chapter 4 evaluates applicability of AWORe for precipitation observation and PWS evaluation. Chapter 5 discusses conclusions and further development opportunities.

2 Precipitation observation

This chapter introduces precipitation formation mechanisms as well as precipitation types and automatic precipitation observation methods. In addition, video recording of precipitations is discussed. Section 2.1 introduces precipitation phenomenon. Section 2.2 presents currently used automatic precipitation observation methods and performance evaluation methods of PWSs. Section 2.3 discusses video recording of precipitations.

2.1 Precipitation

Precipitation is ordinary phenomenon occurring globally. Precipitation occurs in numerous different forms, including rain and snow. The occurrence of different precipitation types varies globally and not all precipitation types are occurring at all locations. Precipitation is always water and it composes in clouds, which are formed as temperature of rising warm air mass reaches dew point. Dew point is temperature where air saturates. Air saturation means that relative humidity has increased to 100 % and water vapor condensates. Water vapor condensates forming liquid droplets when temperature is above 0 °C and composes essentially frozen particles at subzero temperatures. Droplets form around condensation nuclei, such as dust or air pollution particle. Formed droplets collide with other droplets in a cloud and merge to bigger droplets. The droplets begin to fall, when they weight more than air resistance is able to uplift. Precipitation clouds have three distinct mechanisms to form. Cloud types are convective, orographic and stratiform. [3] [4]

Convective clouds occur when air temperature increases as the sun heats ground. As air temperature increases, water evaporation accelerates increasing absolute humidity in the air. Warm and moist air rises higher, where temperature is lower. Due to the decreasing temperature, relative humidity increases and eventually reaches dew point. As the dew point is reached, water vapor starts to condensate forming convective clouds. Convective clouds are forming locally and are horizontally limited, but vertically extensive [4]. Therefore, rain showers from convective clouds are occurring on a relatively small area and are typically short lasting. In Finland, convective precipitations are occurring only in summer. Formation of convective clouds is present in Figure 1. [3]

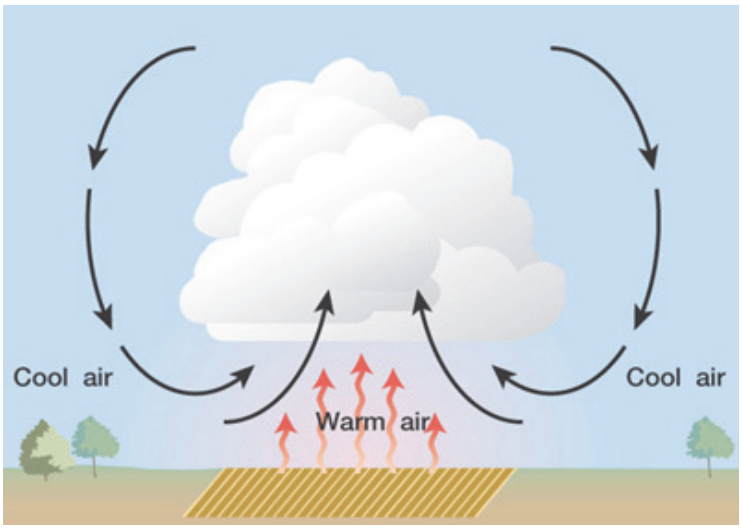

Figure 1. Formation of convective clouds [5]

Orographic precipitations occur mostly on mountains where moist airflow collides to a mountain and forces air mass to rise. As the air mass rises, temperature decreases and moist air saturates starting to form droplets. Precipitation typically remains on a windward side of the mountain and dry air flows to a leeward side as shown in Figure 2. [6]

Figure 2. Orographic precipitation [6]

Stratiform precipitation forms when warm and cold fronts collide, as shown in Figure 3. As the fronts collide, warm air mass rises above the cold air mass, due to the difference in air densities between cold and warm air. The rising air mass cools and reaches dew point, starting the condensation of water vapor. Stratiform clouds are extending to a large area unlike convective clouds. Correspondingly, stratiform clouds are thin whereas convective clouds are thick. Stratiform precipitation is the most common precipitation form in Finland. It is the only occurring precipitation form in winter, when convective clouds cannot be formed due to the low temperature. [3] [4]

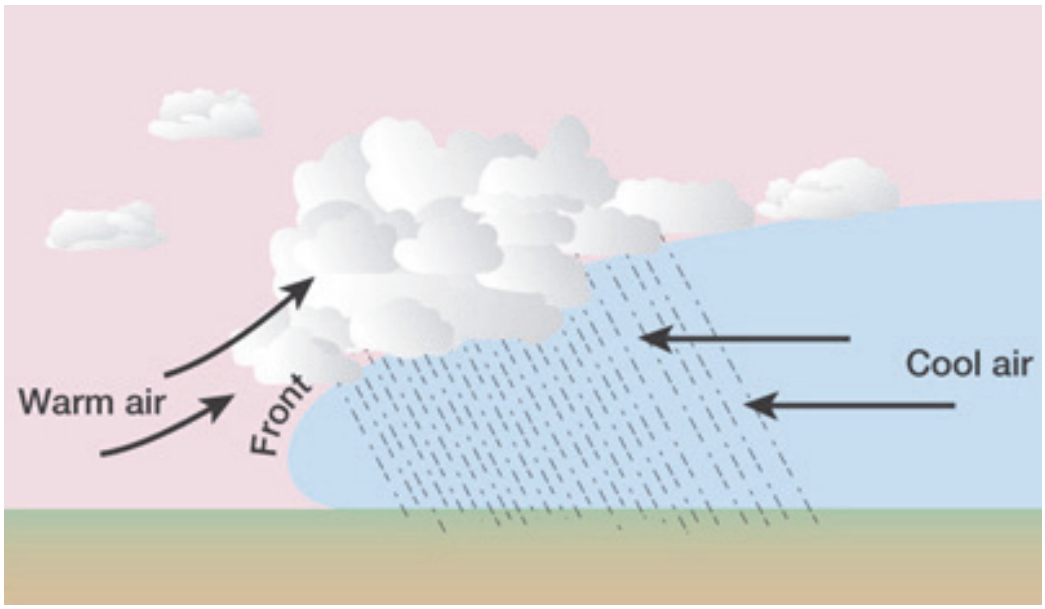

Figure 3. Stratiform precipitation [5]

Precipitation occurs in numerous different types and the occurring type depends on, e.g., vertical temperature profile. The occurrence of different precipitation types significantly varies globally. Precipitation can be divided into three classes: liquid, freezing and frozen precipitation. Different precipitation types are presented in Table 1.

Table 1. Precipitation types. [3] [7] [8]

Liquid precipitations	**Freezing precipitations**	**Frozen precipitations**
Rain	Freezing rain	Hail
		Snow
	Freezing drizzle	Snow grains
Drizzle		Snow pellets (graupel)
	Rain and snow mixed (sleet)	Ice pellets
		Ice crystals

Liquid precipitation types are rain and drizzle. Rain consists of liquid hydrometeors whose diameter is typically 0.3 - 5 mm [3]. Hydrometeor is defined as “any liquid or solid particle formed in atmosphere that is falling from clouds or blown by wind from the ground” [9]. Raindrops are in liquid or frozen form in clouds, but are always in liquid form at ground level. Frozen drops melt when they fall through warm air layer beneath the clouds. Rain originates typically from frozen droplets in Finland [3].

Unlike rain, drizzle originates always from liquid droplets. Drizzle forms in low stratiform and stratocumulus clouds. It consists of small droplets whose diameter is typically 0.3 mm. Although drizzle droplets are typically smaller than rain droplets, distinguishing between these two types cannot be based only on the droplet size, since occurrence of smaller than 0.5 mm raindrops is not exceptional [10]. However, drizzle droplets are more uniform and amount of falling droplets is higher, which distinctly differentiates drizzle from rain. Drizzle originating from stratiform clouds often resembles fog. Stratiform clouds do not extend to the ground contrary to fog, which typically floats slightly above the ground. [3]

Freezing rain consist of supercooled hydrometeors falling in liquid form. Supercooling is a phenomenon where water temperature decreases below its freezing point remaining in liquid form. Liquid droplets require seed crystal to crystalize, i.e., to freeze to a solid particle. Freezing rain and other freezing precipitation types typically require a specific vertical air profile to form. Characteristics of the vertical profile are shown in Figure 4 below. [7]

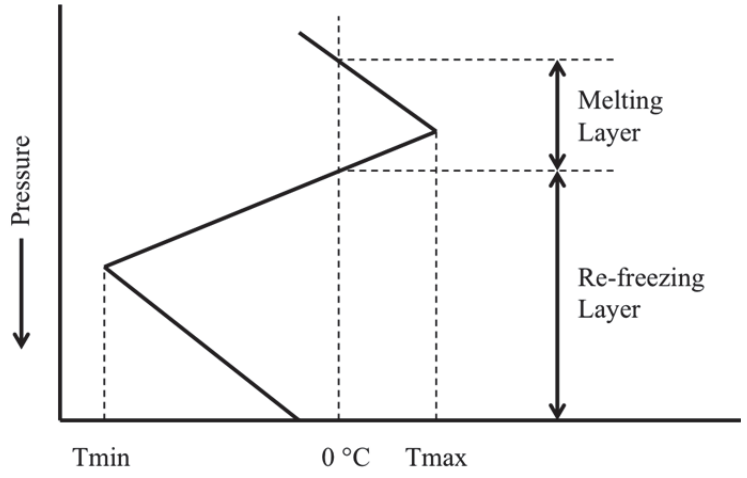

Figure 4. Vertical profile typically occurring during freezing precipitations [7]

As shown in Figure 4, air is stratified into two layers beneath the clouds. The upper layer is warm air layer called the melting layer. The lower layer is cold air layer called the re-freezing layer. Freezing rain originates typically from frozen particles, which melt completely when they fall through the melting layer. Melted droplets fall through the re-freezing layer and become supercooled, as they do not have enough time to freeze in the air before hitting the ground or any other surface close to ground. [7]

Freezing rain may also occur without presence of the presented vertical air profile. Existence of thin supercooled water layers at the top of the clouds were observed already in measurements in 1983 [11]. It is known currently that some clouds are formed mostly of supercooled droplets [12].

These supercooled droplets remain in liquid form during their journey to the ground. Freezing raindrops freeze immediately as they contact a surface, coating the surface with ice. Ice coating makes roadways extremely slippery deteriorating the road safety. Freezing rain is also hazardous for aircrafts, whose ice protection systems are insufficient to protect aircrafts from ice accumulation caused by freezing rain or freezing drizzle. [13]

In Finland, freezing rain is quite infrequent event and is observed mostly in January. Freezing rain and freezing drizzle percentage of total precipitation occurred in Finland was only 2 % between September and April in years 1970 – 2001. The 2 % consists mostly of light freezing rain and light freezing drizzle events, whereas percentage of moderate or heavy freezing rain and drizzle observations was only 0.1 %. [12]

Ice pellets are small and clear ice balls, whose size is less than 5 mm. Ice pellets are formed in similar conditions as freezing rain. They are formed when frozen hydrometeors are melting partially or completely, as they fall from the clouds through the melting layer. The falling hydrometeors are re-frozen in the cold air layer before hitting the ground. [7] [14]

Hail is frozen precipitation, which occurs concurrently with thunderstorms. Hails are small ice balls, which are formed when storm blows liquid droplets higher in the cloud where temperature is lower freezing the droplets. Hail may soar several times up in the cloud and every time a new ice layer is formed on the surface of the hail. Hail size increases as a new ice layer is composed. Thus, hail size indicates the severity of occurring thunderstorm. [14]

Snow is frozen precipitation formed of ice crystals. Ice crystals merge in the cloud composing differently sized and shaped snowflakes. The shapes of snowflakes differentiate them clearly from other frozen precipitation types. Snow pellets are also a form of frozen precipitations. Snow pellets are small white frozen particles formed, when supercooled water droplets are frozen in the air. Snow pellets are also called graupels. The size of snow pellets is less than 5 mm. [15]

Snow grains are significantly smaller than snow pellets. They also remind more ice by being opaque. Snow grains are formed when temperature is low enough to freeze drizzle. Ice crystals are occurring during very low temperatures. Ice crystals are formed as single fog droplets are frozen due to the very low temperature. [15]

It is known that the size and terminal velocity of hydrometeors are well correlated. This was experimentally studied in 1949 [16]. These experiments concentrated only to rain and drizzle droplets. However, the size and terminal velocity correlation of other hydrometeors were studied later and are currently known [17].

Terminal velocity is constant vertical velocity of an object, such as hydrometeor, falling through the atmosphere. Terminal velocity is dependable on two different forces: the gravitational force and drag. The gravitational force causes the falling of the hydrometeor, whereas the drag resists the gravitational force. Drag is dependable on several factors, including air density and drag coefficient. Terminal velocity is reached when the drag is equal to the gravitational force. [18]

The correlation between the terminal velocity and size of a hydrometeor can be utilized in precipitation type classification. By measuring the hydrometeor size and terminal velocity and determining the state of the hydrometeor, the precipitation type can be classified with reasonable accuracy. Terminal velocity distribution for different precipitation types is presented in Figure 5 below.

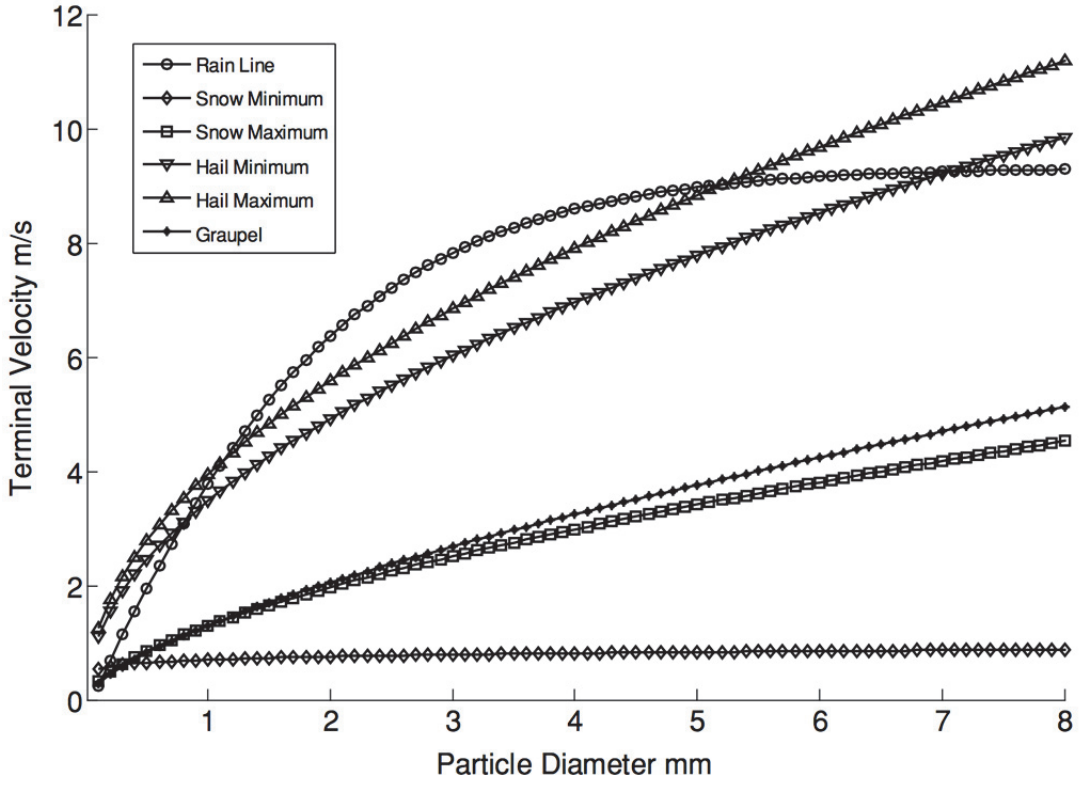

Figure 5. The terminal velocity distribution of hydrometeors [17]

It can be seen from Figure 5 that as the hydrometeor diameter increases, terminal velocity does not increase linearly. Curves of frozen droplets are closer to linear line than curves of liquid droplets. Liquid droplets are essentially spherical, due to water surface tension. However, in certain circumstances droplets are reshaped.

A droplet remains in spherical shape, if the inside pressure of the droplet is stronger than extrinsic pressure affecting it. The inside pressure of the droplet depends on the droplet diameter and water surface tension, which is temperature dependent. Smaller droplets have higher inside pressure and thus, large droplets are more sensitive for extrinsic pressure changes. As large droplets are not spherical, drag increases decreasing their terminal velocity. [19]

Since the terminal velocity of hydrometeors is highly dependable on the hydrometeor size, it is essential to know the precipitation drop size distribution in Finland. All types of precipitation may occur in Finland, due to wide temperature range. However, rain droplets have the steepest slope in Figure 5, i.e., terminal velocity of rain droplets increases most rapidly with respect to the size. In addition, the terminal velocity of hails is high compared to other precipitation types. Nevertheless, hail is infrequent precipitation in Finland, whereas rain is very frequent. Thus, it is essential to know particularly the size distribution of rain droplets. The size distribution of raindrops in Finland determined by radar measurement is presented in Figure 6.

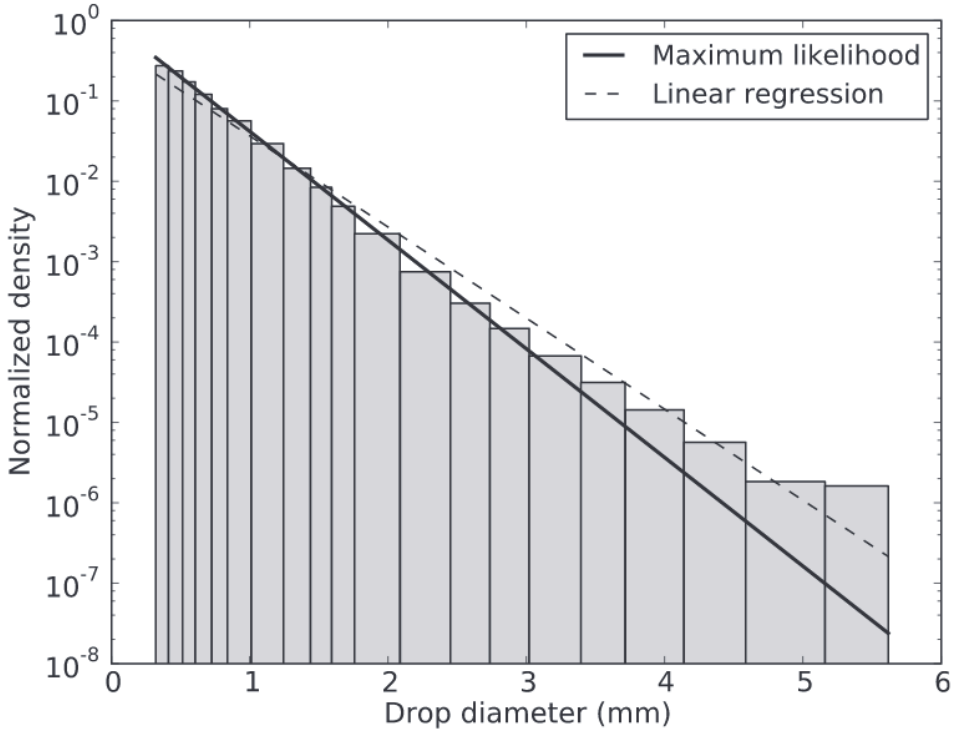

Figure 6. The size distribution of raindrops in Finland [20]

It can be seen from Figure 6 that smaller than 2 mm droplets are more frequent than the droplets larger than 2 mm. Figures 5 and 6 indicate that the typical terminal velocity range of raindrops in Finland is approximately 0.5 – 8 m/s, whereas hydrometeors with higher terminal velocity than 8 m/s are quite infrequent.

2.1.1 Present weather

Present weather is defined as “a description of occurred weather at the time of observation” by World Meteorological Organization (WMO) [9]. Present weather information typically consists of precipitation and obscuration parameters. Since present weather parameters are not defined, used present weather parameters vary. Precipitation parameters often included are the following: precipitation type, accumulation, intensity and character. This information is vitally important in fields, where some precipitation types increase significantly risk of an accident. For example, freezing precipitations are extremely hazardous in aeronautics and has caused several accidents [13]. Consequently, the occurrence of freezing precipitations must be detected so that aircraft pilots are aware of occurring hazardous conditions.

Observing of present weather is challenging and professional human observers provide the most precise results regarding to classification of precipitation types. However, utilization of PWSs has increased during last decades and partially replaced human observers. Advantages of PWSs compared to human observers are decreased demand of resources and increased objectivity in observations. The major disadvantage is the varying reliability of PWSs between different precipitation types (Section 2.2.1).

Present weather is typically presented using various code systems. In aeronautics, present weather is presented in Aviation Routine Weather Reports (METAR), which is processed every hour. METAR consists of 11 parts in its entirety, containing general information and weather information.

Present weather information in METAR is composed of two parts: qualifier and weather phenomena. The qualifier indicates occurring intensity and character, whereas weather phenomena indicate precipitation type or obscuration. The construction of the present weather code in METAR is shown in Table 2.

Table 2. Present weather code construction in METAR. [21]

Qualifier				**Weather Phenomena**					
Intensity or Proximity		**Descriptor**		**Precipitation**		**Obscuration**		**Other**	
–	Light	BC	Patches	DZ	Drizzle	BR	Mist	DS	Dust- storm
		BL	Blowing	GR	Hail	DU	Wide-spread Dust		
	Mode-rate	DR	Low Drifting	GS	Snow pellets	FG	Fog	FC	Funnel Clouds
		FZ	Freezing	IC	Ice Crystals	FU	Smoke	PO	Dust/ Sand Whirls
+	Heavy	MI	Shallow	PL	Ice Pellets	HZ	Haze	SQ	Squall
		PR	Partial	RA	Rain	SA	Sand		
VC	Vici-nity	SH	Shower	SG	Snow Grains	VA	Volcanic Ash	SS	Sand-storm
		TS	Thunder -storm	SN	Snow				

It can be seen from Table 2 that intensity is presented using + and – characters. Intensity limits depend on the precipitation type and are shown in Table 3.

Table 3. Intensity limits used in METAR and NWS code. [8]

METAR/SPECI/NWS Intensities [mm/h]	**Light**	**Moderate**	**Heavy**
Drizzle	≤ 0.25	> 0.25 ... 0.5	> 0.5
Rain, drizzle with rain, sleet, precipitation	≤ 2.5	> 2.5 ... 7.6	> 7.6
Snow, snow pellets, snow grains, ice pellets	≤ 1.25	> 1.25 ... 2.5	> 2.5

Another form of METAR is called SPECI and is established whenever significant change in weather conditions is observed. Such a change can be, e.g., significant change in visibility.

Other commonly used code for presenting present weather is defined by National Weather Service (NWS). NWS code consists of precipitation type and intensity information. NWS codes and corresponding precipitation types are presented in Table 4.

Table 4. NWS code table for precipitation types. [8]

Precipitation Type	**NWS Code**
No Precipitation	C
Precipitation	P
Drizzle	L
Rain	R
Snow	S
Rain and drizzle mixed	RL
Rain and/ or snow mixed	RLS
Freezing drizzle	ZL
Freezing rain	ZR
Ice pellets	IP
Snow pellets	SP
Snow grains	SG
Hail	A
Ice crystals	IC

Intensity is presented in NWS code similarly as in METAR (Table 3). PWSs are typically reporting at least one of the presented codes. PWSs are presented in more detail in Section 2.2. [9]

2.2 Automatic precipitation observation methods

Trained weather observers have classically performed all weather observations, including precipitation observations. However, AWOSs have been utilized in precipitation measurements for decades already. Nevertheless, AWOSs have not completely replaced human observers. The need of human observers emphasizes to visual observations, such as classification of precipitation types [9]. However, human observers utilize also measurement data from AWOSs in precipitation observations [22]. AWOSs typically measure the following parameters [23]:

- air temperature
- precipitation
- present weather
- clouds
- pressure
- visibility
- humidity
- wind
- solar radiation
- sunshine.

Weather parameters listed above are fundamental weather parameters that are used for numerous purposes. Most of these parameters are beneficial for precipitation type classification. Precipitation observation contains fundamentally four objects: precipitation type, character, intensity and accumulation [9]. Precipitation types were presented in Section 2.1. Precipitation character is determined into one of the following: showers, intermittent precipitation or continuous precipitation. Precipitation intensity can be expressed, e.g., as millimeters per hour. In some cases, intensity is presented in three categories, as introduced in Section 2.1.1. Precipitation accumulation determines the amount of precipitation accumulated at a certain time range.

Precipitation intensity and accumulation are measured often by precipitation gauges. Precipitation gauges are able to measure intensity and amount of few different precipitation types. For example, OTT Pluvio² precipitation gauge is capable to measure intensity and accumulation of rain, snow and hail [24]. Gauges measuring only liquid precipitations are designated rain gauges. Two different precipitation gauge types are commonly used.

The most accurate gauge type is weighing gauge. Weighing gauge collects all precipitation from a specific area and measures the weight of the collected precipitation. The weight gives the amount of precipitation and by considering the time simultaneously with the weight, precipitation intensity and accumulation can be determined. [9]

Other commonly used gauge type is tipping bucket. The tipping buckets collect precipitation from a specific area similarly as weighing gauges. Instead of measuring the weight of collected precipitation, tipping bucket calculates the number of tips a balance in the bucket does. The balance has cups on its both ends. One cup is filled at a time and as the cup contains a specific amount of water, the balance tips. [9]

PWSs have been used for decades in precipitation measurements as well. PWSs are measuring precipitation type, intensity and accumulation. The utilization of PWSs emphasizes in visual observations, such as precipitation type classification, as the other precipitation measurement methods are also able to measure intensity and accumulation accurately [9]. Consequently, PWSs are used mostly in the environments where precipitation type and visibility information is crucial. Although the sensors are relatively precise for classifying of certain precipitation types, some precipitation types are weakly or never detected. Precipitation type classification methods used by PWSs are presented in Section 2.2.1.

2.2.1 Principles of automatic hydrometeor classification

Currently, mainly PWSs are used in automatic hydrometeor classification. PWSs are used widely in different environments, including roadways and runways. In addition to hydrometeor classification, PWSs are measuring also other present weather parameters, including visibility, precipitation intensity and accumulation. The sensors utilize several concurrent measurements to determine the parameters. The primary measurement is optical measurement, based typically on scattering of light. Other measurements are used to assist the optical measurement in hydrometeor classification. One commonly used assisting parameter is temperature. Further developed PWSs perform more measurement, such as wetness measurements. Four different PWS models from different manufacturers are shown in Figure 7. [9] [22]

Vaisala PWD52

Biral VPF-710

Campbell Scientific PWS100

Belfort 6550

Figure 7. Four present weather sensor models [25] [26] [27] [28]

PWSs have utilized practically two different optical measurement principles over time. First measurement principle analyzes fluctuation of infrared beam occurring during precipitation. For example, Light Emitting Diode Weather Identifier (LEDWI) used in Automated Surface Observing System (ASOS) utilizes this measurement principle. LEDWI contains transmitter that transmits thin and relatively wide laser beam toward a receiver of the sensor. The receiver uses photodiode to detect the intensity of the transmitted beam. As a hydrometeor falls through the transmitted beam, a short peak appears in the received signal. When several droplets fall through the beam sequentially, several peaks occur in the signal creating a pattern. The sensor analyzes the frequency of the pattern to distinguish between rain and snow. LEDWI utilizes also other parameters for distinguishing between rain and snow. However, this measurement principle is not able to identify any other precipitation types than rain and snow. The sensor is able to determine precipitation intensity when only one type of precipitation is occurring at a time. [22] [29]

Second and the most common principle, is forward scatter principle. In forward scatter principle, intensity of scattered light toward the receiver is measured. Forward scatter principle has been found to be suitable principle for hydrometeor classification, whereas the first introduced principle has been found to be suitable only for precipitation detection. [22]

PWSs utilizing forward scatter principle are typically fundamentally visibility sensors that measure scattering coefficient and utilize that for determination of the extinction coefficient. In simplified models, extinction coefficient is typically assumed to be equal to scattering coefficient when water particles are considered. This is due to insignificant absorption factor, as the visibility decreases during precipitation, due to reflection, refraction or diffraction. Light interaction with round droplets presented in Figure 8. [9] [30]

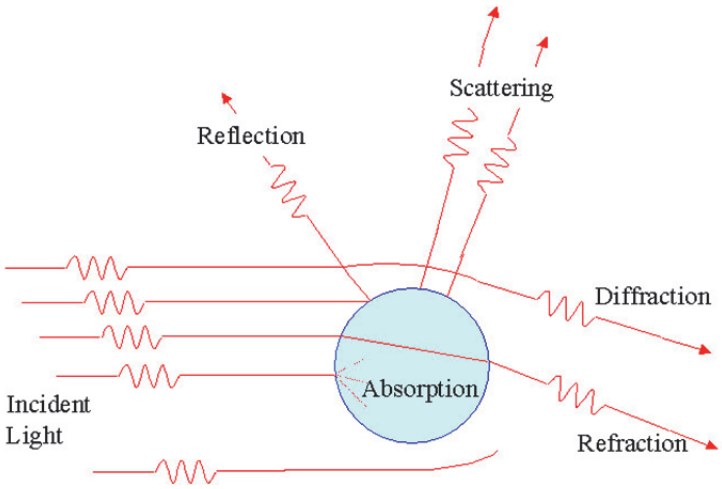

Figure 8. Light interaction with a round droplet [31]

Extinction coefficient is fundamental parameter in visibility measurements and is used for determining other visibility quantities as well. Visibility sensors often report visibility in Meteorological Optical Range (MOR), which indicates the transparency of atmosphere. MOR is defined as "a distance in the atmosphere required to reduce the luminous flux in a collimated beam from an incandescent lamp, at color temperature of 2700 K, to 5 % of its original value" [32].

In aeronautics, other commonly used quantity for visibility is Runway Visual Range (RVR). RVR is defined, as a horizontal distance a pilot in an aircraft on a runway is able to see the runway lights or markings. Regulations of International Civil Aviation Organization (ICAO) require all airports to calculate local RVR. ICAO authorizes international airport regulations. [33]

Most of the PWSs use optical arrangement presented in Figure 9. However, the angle of the transmitter and receiver varies in different sensors. The recommended scattering angle is 20 - 50 °. It has been found that the scattering angle of 42 ° gives equal fog and snow calibration. The tilt should be also down to avoid contamination of lenses. [30]

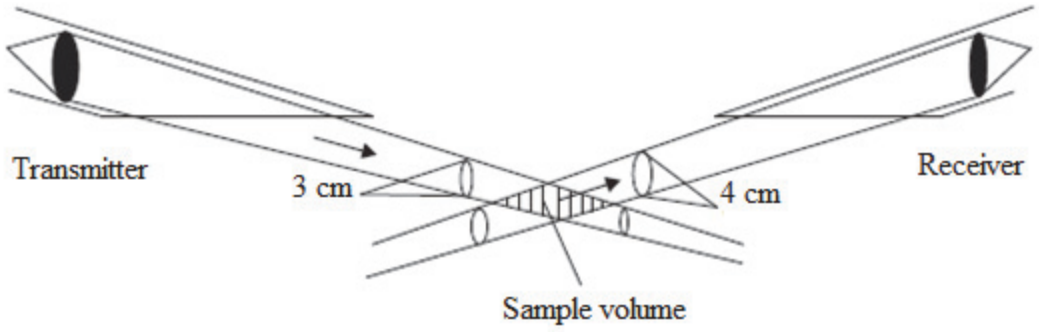

Figure 9. Optical arrangement of Vaisala PWDs [34]

The intensity measurement is performed so that the transmitter transmits infrared beam toward sample volume. The wavelength of the beam used is typically 830-900 nm. The incident light scatters as hydrometeors fall through the sample volume and the receiver detects the intensity of scattered light by using photodiode. The sample volume is often relatively small. For example, Vaisala PWD52 sample volume is approximately 0.1 liters. Small sample volume is advantageous when individual droplets are required to be identified during heavy precipitations. Small sample volume also enhances the detection of smallest precipitation droplets. [34]

The intensity measurement data is also used to classify hydrometeors. As intensity of scattered light depends on hydrometeor size, the hydrometeor size can be determined from the measurement data. By analyzing intensity measurement data, terminal velocity of the hydrometeor can also be determined.

Mie scattering theory applies for hydrometeors whose size is close to wavelength of incident light, such as fog droplets. Typical fog droplet size is between 1 and 64 microns, which is close to used wavelengths of 830 - 900 nm [35]. Larger hydrometeors are scattering light differently, as they behave as refractors and reflectors [34]. Refraction of the incident light was illustrated in Figure 8.

Individual hydrometeors are detected by detecting amplitude changes in the received signal. As PWSs continuously measure intensity of scattered light, they detect all changes in the scattering intensity. When a large hydrometeor falls through the sample volume, a peak appears in the received signal. The amplitude of the peak in the signal is proportional to the size of the detected hydrometeor. By analyzing amplitudes of peaks, the hydrometeor size can be determined. The hydrometeor size is proportional to precipitation intensity, allowing estimation of the intensity as well. The width of the peak is proportional to the terminal velocity of the hydrometeor. Hence, the terminal velocity can be determined by analyzing the same signal. [34]

In addition, other precipitation type classification methods are applied. For example, Campbell Scientific PWS100 sensor utilizes two receivers. The sensor algorithm considers received signal of both receivers, A and B. By calculating the time difference between the signal changes, terminal velocity of the hydrometeor can be determined. [17]

As described earlier in this section, PWSs using forward scatter technology utilize several parameters in precipitation identification, including temperature. For example, Vaisala PWD52 includes temperature and capacitive rain sensor. The rain sensor is designed to detect only liquid form precipitation. However, the sensor is heated melting frozen particles falling on it. The rain sensor assists to distinguish between frozen and liquid precipitation types. An algorithm considers temperature and rain sensor data alongside forward scatter measurements to determine occurring precipitation types. [34]

PWS algorithms typically use threshold values, which exclude some precipitation types when exceeded. One limit can be, e.g., temperature. If temperature is higher than 8 °C, the occurring precipitation cannot be snow and detected precipitation is considered as rain. A flowchart of an example algorithm is presented in Figure 10. [22]

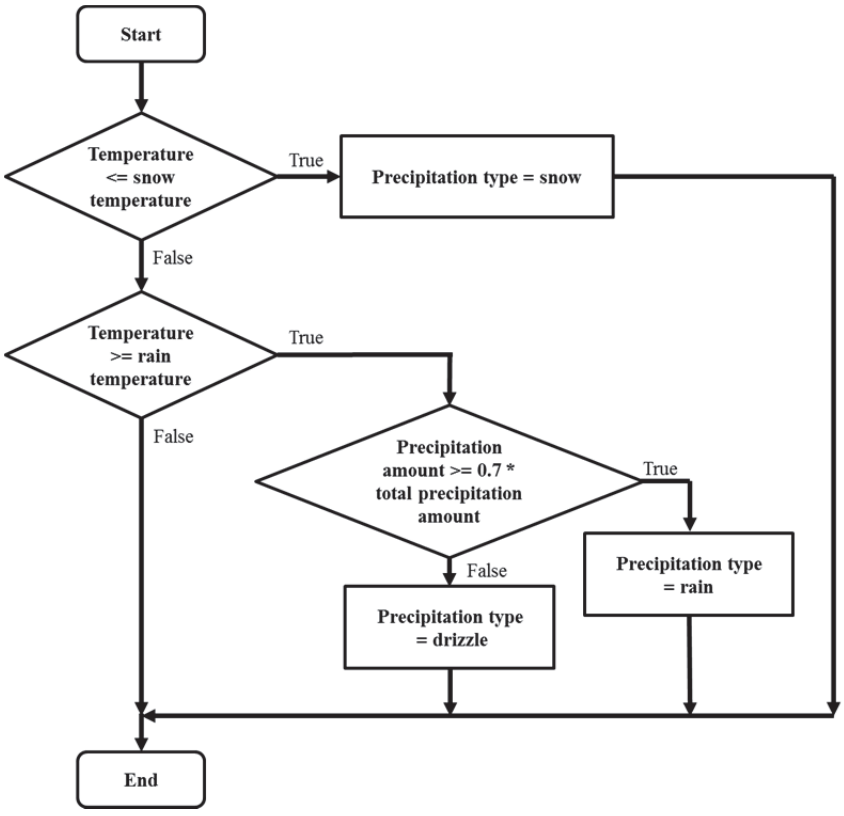

Figure 10. PWS algorithm example [22]

The flowchart describes simplified PWS algorithm. The algorithm considers current temperature and if the temperature is lower than snow temperature, precipitation is determined to snow. If the temperature is higher than snow temperature, algorithm checks whether the temperature is lower or higher than rain temperature.

If temperature is higher than rain temperature, the algorithm considers precipitation amount information. In case, the amount of the precipitation is more than the threshold value, precipitation is classified to rain. If the threshold value is not exceeded, precipitation is classified to drizzle. Current PWSs are unable to recognize all precipitation types. Precipitation types that the current PWSs are typically able to recognize are listed below:

1. rain
2. drizzle
3. snow
4. mixed rain/snow
5. freezing rain
6. freezing drizzle
7. ice pellets
8. snow pellets.

Some PWSs report even more precipitation types than listed. However, not all PWSs are able to recognize all of the listed precipitation types. Moreover, PWSs have several identified problems in precipitation type classification. Problems relate mostly to light and mixed precipitations. For example, drizzle is generally weakly identified by PWSs. In addition, PWSs are usually unable to classify the precipitation type during light precipitation events. In case of mixed precipitations, PWSs are typically reporting only one of the occurring precipitation types. [22]

2.2.2 Evaluation methods of present weather sensors

In recent decades, PWSs have increasingly replaced human observers. Correspondingly, attention given for performance evaluation methods of PWSs has increased, since the reliability of PWSs is the major barrier for replacing human observers by PWSs. This section presents commonly used methods for performance evaluation of PWSs. Methods to be presented focus on precipitation type classification. Methods used for evaluation of precipitation intensity and accumulation measurements are not discussed in this section, since this thesis focuses on classification of precipitation types.

Evaluation of PWSs is challenging, due to the subjectivity of the phenomena [1]. Essentially, two different evaluation methods are used:

- Intercomparison between human observer and PWS.
- Intercomparison between PWSs.

Intercomparison between PWSs is simpler method and generally requires less effort than intercomparison between human observers and PWS, since human observers are not required to be present during the evaluation period. Observers or other professionals are needed only in data analysis after the evaluation period. However, this method does not indicate the probability of PWSs to report correct condition. Only the consistency of the PWSs under evaluation can be determined using this method. Although determining the probability of the PWSs to report correct condition using this method is not possible, the consistency of the PWSs is vital information for PWS manufacturers, making this method also beneficial.

Intercomparison between human observer and PWS is the only reliable method for performance evaluation of PWSs, since human observations are used as a reference [1]. Consequently, this evaluation method requires more resources, since human observers must be present during the whole evaluation period. In practice, this often leads to situation where the evaluation is performed only during daytime. Moreover, evaluation periods should be relatively long, as some precipitations types are very infrequent.

In intercomparison between human observer and PWS, four different event types may occur and the count of each event type is determined. The four event types are [36]:

a. Human observer and PWS report the same event.
b. Only human observer reports the event.
c. Only PWS reports the event.
d. No event reported.

The goal in evaluation is to determine verification scores for the PWS under evaluation utilizing the count of each event type. For example, the following verification scores could be used in evaluation of PWSs [36]:

- Probability of Detection (POD)
- False Alarm Ratio (FAR)
- Critical Success Index (CSI)
- Heidke Skill Score (HSS)

The POD determines the probability of PWS to report correct condition and can be calculated by [36]

$$\mathrm{POD} = 100\ \% \ \frac{\mathrm{a}}{(\mathrm{a} + \mathrm{b})}, \tag{1}$$

where a and b are the counts of corresponding event types. As can be seen from Equation 1, the POD indicates the performance of PWS quite well. However, the POD does not consider the number of false alarms. The FAR determines the probability of the PWS to give false alarm. The FAR can be calculated as follows [36]:

$$\mathrm{FAR} = 100\ \% \ \frac{\mathrm{c}}{(\mathrm{c} + \mathrm{d})} \tag{2}$$

The FAR is particularly important quantity for fields, where executing of certain operations depend on the PWS report, since it is not beneficial to stop operations, due to a false alarm. The CSI is similar to POD with the difference that the CSI considers also the number of false alarms. The CSI is expressed such that [37]

$$\mathrm{CSI} = 100\ \% \ \frac{\mathrm{a}}{(\mathrm{a} + \mathrm{b} + \mathrm{c})} \tag{3}$$

The CSI indicates the performance of PWS very extensively and is thus, important score. The HSS is widely used in weather forecasting and is also utilized in PWS evaluation. The HSS indicates how well a PWS performs compared to a human observer. The HSS corrects the result with a random chance and can be calculated as follows [36]:

$$\mathrm{HSS} = 100\ \% \ \frac{(\mathrm{ad} - \mathrm{bc})}{(\mathrm{ad} - \mathrm{bc}) + \frac{1}{2}\mathrm{n}(\mathrm{b} + \mathrm{c})} \tag{4}$$

, where n is the sum of all events. Determination of the presented verification scores indicates the reliability of the PWS under evaluation very well. However, incorrect reports of PWSs often relate to certain precipitation types, such as hail or mixed precipitations. Thus, it is essential to consider precipitation types occurred during the evaluation period. It is typical for PWS evaluation that only liquid or frozen precipitation types are considered within one evaluation period [1]. However, the best evaluation results are achieved when all precipitation types are considered in determination of verification scores.

2.3 Video recording of hydrometeors

Recording of fast objects, such as hydrometeors, is more demanding than recording of still objects. Both, video recording and photography have same principles in the recording of fast objects. Recording of hydrometeors requires always very short exposure time. One additional parameter to be considered in video recording is frame rate. Frame rate is expressed as frames per second (fps).

Insufficient exposure time affects motion blur appearing on recorded video. Motion blur determines the amount of blur around the recorded object to due to the movement of the object. The motion blur appears only in the direction of the movement. A simplified estimation of the motion blur can be calculated by:

$$\text{Motion blur} = v_{object} \times t_{exposure}, \quad (5)$$

where v_{object} is the velocity of an object and $t_{exposure}$ is the exposure time [38]. It can be seen from Equation 5 that faster objects require shorter exposure time to retain the same motion blur. As shown earlier in Figure 5, the terminal velocity of hydrometeors can be over 10 m/s.

The required exposure times to clearly display hydrometeors depends on the terminal velocity of hydrometeors. The acceptable motion blur depends always on the displayed object. In order to achieve the motion blur of 0.5 mm, which is assumed in this thesis to be sufficient for hydrometeors, exposure time must be adjusted as presented in Table 5.

Table 5. Required exposure times to achieve motion blur of 0.5 mm.

Hydrometeor size [mm]	Motion blur [mm]	Snow terminal velocity	Rain terminal velocity	Hail terminal velocity	Snow Texp [us]	Rain Texp [us]	Hail Texp [us]
0.1	0.5	0.2	0.2	1.2	2500.0	2500.0	416.7
1	0.5	1.3	3.6	3.9	384.6	138.9	128.2
2	0.5	1.8	6	5	277.8	83.3	100.0
3	0.5	2.5	7.8	6.8	200.0	64.1	73.5
4	0.5	3	8.5	7.8	166.7	58.8	64.1
5	0.5	3.5	9	8.8	142.9	55.6	56.8
6	0.5	3.9	9.1	9.7	128.2	54.9	51.5
7	0.5	4.2	9.2	10.5	119.0	54.3	47.6
8	0.5	4.8	9.4	11.3	104.2	53.2	44.2

Values presented in Table 5 are calculated using Equation 5 and the terminal velocity values are estimated from Figure 5. It can be seen from Table 5 that the shortest exposure time required is approximately 44 us. Available exposure time depends on the shutter speed of a camera. Currently, many high-speed cameras have shutter speed of 1/20 000 or faster. However, HSCs with faster shutter speeds costs more when the price may become an obstacle.

When exposure time is decreased, higher illuminance is required. Required illuminance is often estimated using exposure value (EV). EV is dependent on aperture f-number N and exposure time $t_{exposure}$ such that [39]

$$EV = \log_2 \frac{N^2}{t_{exposure}} \tag{6}$$

Aperture f-number can be expressed as a relation of a focal length and aperture diameter as follows [40]:

$$\text{f-number} = \frac{\text{Focal length}}{\text{Aperture diameter}} \tag{7}$$

When f-number is increased by one stop, twice as much light is required to retain the same exposure level in the image. In order to allow twice as much light in, the aperture area must be doubled. F-number stops increase by steps of $\sqrt{2}$ in standard aperture size series, as presented in Equation 8 [41].

$$f/1.0 = \frac{f/1.4}{\sqrt{2}} \tag{8}$$

In addition, aperture size affects depth of field (DoF), which determines the distance between near and far sharp points [39]. DoF increases as f-number increases and can be expressed as follows [42]:

$$DoF = T_r + T_F, \tag{9}$$

where T_r and T_F are the backward and forward DoFs, respectively.

These two parameters can be calculated by

$$T_r = \frac{\delta f L^2}{F^2 - \delta f L}$$
$$T_F = \frac{\delta f L^2}{F^2 + \delta f L}, \quad (10)$$

where δ is a permissible circle of confusion (CoC), f is f-number, F is a focal length and L is an object distance [42]. Sufficient DoF varies significantly depending on the recorded object. Reasonable DoF to be used in recording of individual hydrometeors is magnitude of centimeters [43]. When requirements for exposure time and DoF are defined, required EV can be estimated from Figure 11.

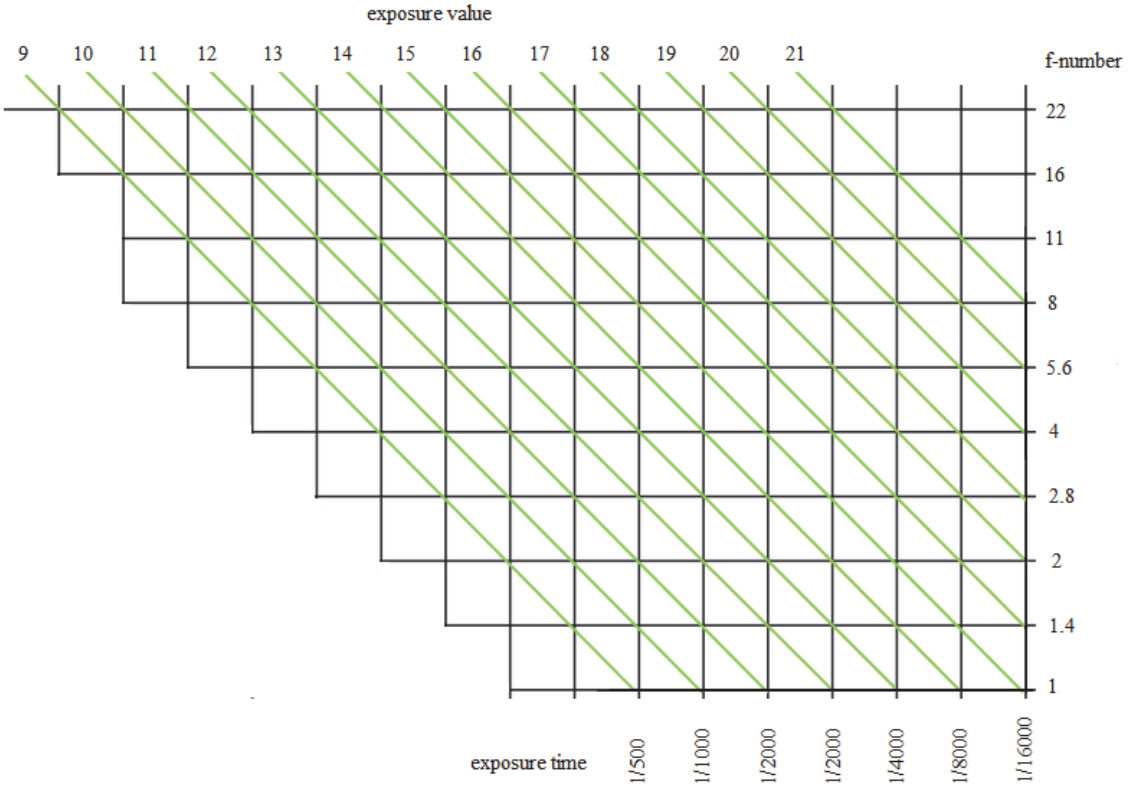

Figure 11. EVs and corresponding exposure time and f-number combinations [39]

As the required EV is known, corresponding illumination value can be estimated from Table 6.

Table 6. Exposure values and corresponding illuminance values. [39]

EV100	**Illuminance [lx]**
10	402
11	804
12	1609
13	3217
14	6434
15	12868
16	25736
17	51472
18	102944

Exposure time, DoF and required illuminance are parameters that must always be considered in photography and video recording. Furthermore, frame rate must be considered in video recording. Frame rate must be matched with the used field of view (FOV). Time between two individual frames must be shorter than the time hydrometeor stays within the FOV. The time between two frames can be calculated as follows:

$$T_{img} = \frac{1}{fps} \tag{11}$$

The time a hydrometeor stays within the FOV is estimated such that

$$t_{pass} = \frac{FOV}{v_{hydrometeor}}, \tag{12}$$

where $v_{hydrometeor}$ is the velocity of the hydrometeor. In order to confidently capture hydrometeors that fall through the FOV of the HSC, a camera must be able to capture two frames in the time t_{pass} shown in Equation 12. Otherwise, in certain situations the hydrometeor might pass the FOV without being captured. Additionally, at least two frames must be captured from an individual hydrometeor in order to estimate the terminal velocity.

Thus, the relation between t_{pass} and T_{img} must be such that

$$\frac{t_{pass}}{T_{img}} \geq 2 \tag{13}$$

Consequently, minimum frame rate can be expressed as follows:

$$fps_{min} = \frac{2}{t_{pass}} \tag{14}$$

When all presented parameters are considered, it can be noticed that typical network cameras used, e.g., in surveillance, are not sufficient for recording of individual droplets. Network cameras have usually fixed, automatically adjusted or insufficient shutter speed, which limits the exposure time and thus, the recording of fast objects is not typically possible. Since network cameras are continuously streaming video, frame rate must be limited to 25 - 30 fps with 1920 x 1080 px resolution to avoid the overload of networks.

Network cameras are sufficient to record a general view of occurring precipitations, since it is not necessary to capture clearly individual hydrometeors. In order to enhance the detection of hydrometeors, network cameras and HSCs require a contrast plate. The contrast plate used with network cameras should be matte black to avoid unwanted reflections. The plate should have markings that assist in hydrometeor terminal velocity and size estimation. The terminal velocity and size estimation methods are presented in Section 2.3.2.

The contrast plate to be used with HSCs can be black or white depending on the used light source and the angle of the transmitted light. The contrast plate used with the HSCs should also have markings to assist in hydrometeor size and terminal velocity estimation.

2.3.1 High-speed video recording

Term high-speed video recording is typically used when considering HSC recordings. HSCs are recording video with higher frame rate than the conventional cameras are capable of. HSCs have evolved in recent decades, increasing their utilization in industry. Additionally, prices of HSCs have decreased. However, the price range of HSCs is still wide. The cheapest HSCs cost hundreds of euros and require PC or other acquisition device to function. They contain no data storage and their features are limited. More expensive HSCs include often data storages and have better features, such as faster shutter speed.

However, the data storages are currently relatively small compared to the video sized. Thus, the data must be frequently transferred from the data storage to an external storage device. HSCs are utilizing further developed technology than conventional cameras to achieve the higher frame rates. HSCs are typically processing images in real-time using integrated processor and sensor chips. Additionally, Field Programmable Gate Array (FPGA) boards are used in image processing. [44]

In order to capture individual hydrometeors, the frame rate must be significantly higher than 25 fps, which is typical frame rate of network cameras. In addition, fast shutter speed is required to achieve short exposure time. It was shown in from Table 5 that required exposure times in the video recording of hydrometeors are close to 100 us. If smaller motion blur would be required, the exposure time should be much lower. Low cost HSCs have typically shutter speed of 1/17 000 or slower. In order to achieve exposure time of 10 us, the shutter speed should be 1/100 000. HSCs with the shutter speed of 1/100 000 or faster are remarkably more expensive. Thus, the price is one of the major factors when a HSC is selected for a recording system.

2.3.2 Terminal velocity and size estimation of hydrometeors

As presented earlier in Section 2.3, individual hydrometeors can be clearly captured using a HSC. It was described in Section 2.1 that the terminal velocity and size of hydrometeors are well correlated. In order to classify precipitation types, the determination of those parameters is necessary. Particularly, the importance of those parameters is emphasized when the precipitation type cannot be reliably classified from the visual appearance of the captured hydrometeor.

The terminal velocity can be estimated from video recordings estimating the moved distance between two consecutive frames. However, this is only possible when the frame rate is known. The time between two frames can be calculated using Equation 11 as described in Section 2.3. For example, with 500 fps the time between two frames would be 2 ms. Two consecutive frames are illustrated as one in Figure 12.

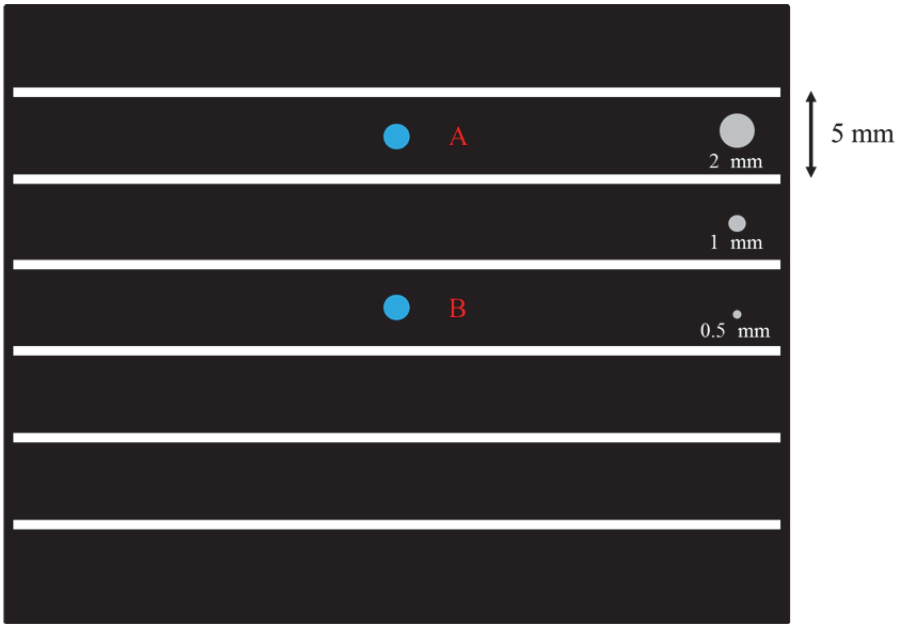

Figure 12. Illustration of terminal velocity and size estimation

The distance between the points A and B can be estimated from the image utilizing the horizontal lines on the background (Figure 12). The distance s was estimated to be 10 mm, when the terminal velocity can be determined as follows:

$$\text{Terminal velocity} = \frac{s}{T_{img}} = \frac{10\ \text{mm}}{2\ \text{ms}} = 5\ \text{m/s} \tag{15}$$

Since 500 fps and distance of 10 mm were used in Equation 15, the terminal velocity was determined to be 5 m/s. The size of the hydrometeor can be estimated by comparing it to the dots on the background of the image. The size of the hydrometeor in Figure 12 was estimated to be 1.5 mm. By comparing the size and terminal velocity of the hydrometeor to the Figure 5, the precipitation type could be identified to rain or hail. However, the visual appearance of the hydrometeor indicates the precipitation type to be rain.

The presented method is suitable for HSC recordings and also for network camera recordings at some extent. However, hydrometeors will occur as stripes in network camera recordings, due to the motion blur caused by long exposure time. Nevertheless, by estimating the moved distance, a rough estimation of the terminal velocity can be made.

Furthermore, the long exposure time has no affection on the width of the stripes, since the motion blur appears only on the direction of the movement. Consequently, the size of hydrometeors can be estimated quite precisely from network camera recordings as well.

3 AWORe development

This chapter introduces materials and methods used in the development of AWORe. Section 3.1 introduces requirements placed for AWORe. Section 3.2 presents comprehensively the components and methods used in the hardware development. Section 3.3 describes AWORe software development process.

3.1 Requirements

The purpose of AWORe is to allow human observers to determine the precipitation occurring at any given time without requiring human observers to be continuously present. In order to reliably determine precipitations, the precipitations must be visually examined. When the precipitation type cannot be reliably classified in visual examination, weather measurement data must be available to assist observers. Since terminal velocity and size of hydrometeors are well correlated (Section 2.1), measuring these parameters assists also in precipitation type classification. In order to provide all necessary material for observers, the following requirements are placed for AWORe:

- AWORe must:
    - enable classification of all precipitation types presented in Table 1
    - allow performance evaluation of PWSs using both methods described in Section 2.2.2
    - have operational temperature range of -40 … +40 °C
    - continuously record video of occurring weather with two network cameras, which must:
        - have 1920 x 1080 px resolution
        - have 25 fps or higher
        - have 20 x optical zoom or higher
        - have IP 66 classification
        - have adjustable preset positions to display different views
    - primary network camera must also:
        - record toward a contrast plate, which must:
            - be size of 660 x 660 mm
            - be installed perpendicularly to the primary camera with slant distance of 3 m

        - have installation height of 1.3 m
        - have matte black background with markings that assist in hydrometeor size and terminal velocity estimation
        - be heated to avoid any precipitation accumulation on its surface
        - be illuminated
        - have collector plate to collect hydrometeors
    - continuously record audio of occurring weather to assists in distinguishing between liquid and frozen precipitations
    - continuously measure sufficient weather parameters presented in Section 2.2, which are:
        - air temperature
        - relative humidity
        - air pressure
        - precipitation intensity
        - precipitation accumulation
        - wind speed
        - wind direction
        - visibility in meteorological optical range
        - cloud height and amount of two cloud layers
    - measure present weather using at least two PWSs utilizing different measurement principles presented in Section 2.2.1
    - have capability to detect changes in present weather
    - have web UI for the insertion of real-time and past weather observations
    - report daily all detected events and include latest values from all sensors at the time of each event
    - have capability to store acquired data for 30 days
    - use a HSC, which must:
        - support 640 x 480 px resolution
        - be able to record video of individual hydrometeors whose maximum terminal velocity is 10 m/s with the motion blur of 0.5 mm or less.

3.2 Hardware development

AWORe is designed according to the requirements presented in Section 3.1. AWORe is required to use two network cameras, a microphone, a HSC, a PC and a network storage array (NAS). These components are main components of AWORe. AWORe must also have a web UI where observers may submit observations. Web UI development is presented in Section 3.3.5. AWORe utilizes wide sensor network, which already exists at Vaisala test field. The sensor network is used to measure basic weather parameters that assist in precipitation type classification. Utilized sensors are presented in Section 3.2.4. A block diagram of AWORe was made to illustrate the construction of AWORe and also to see required connections between different components. The block diagram is shown in Figure 13.

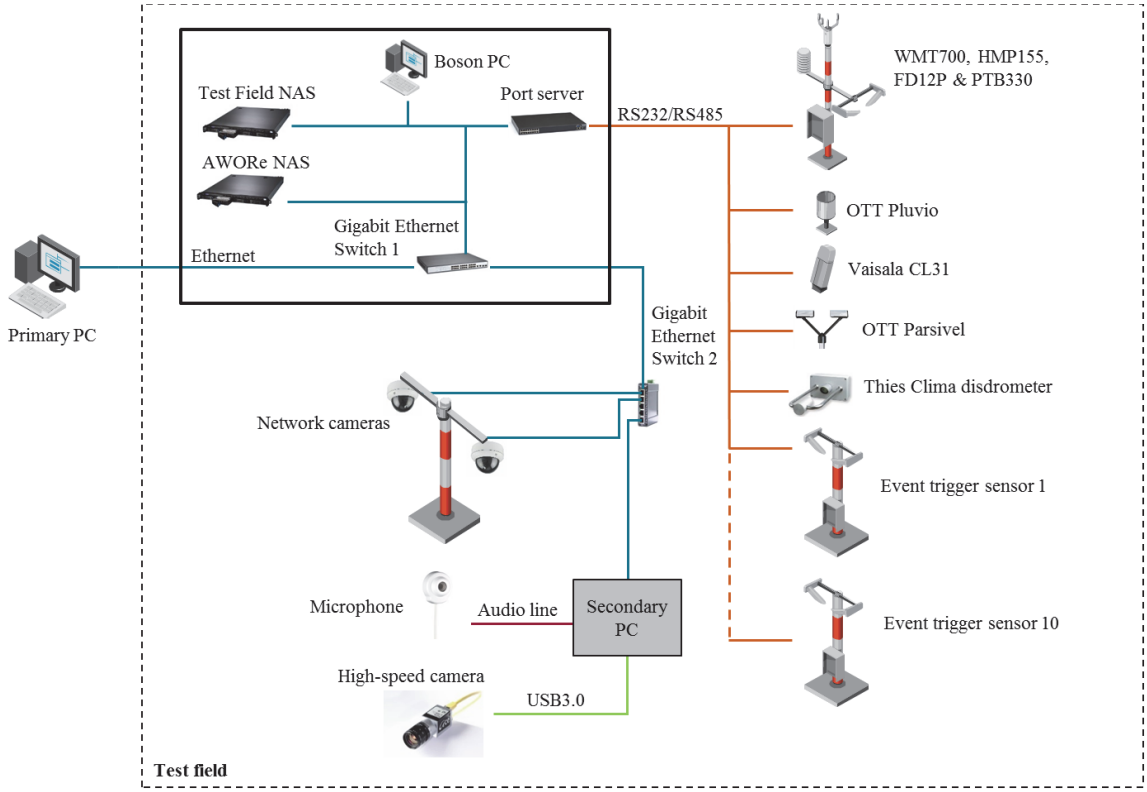

Figure 13. AWORe block diagram

In addition to the sensor network, AWORe utilizes also other components that already existed at Vaisala test field, including Boson PC and test field NAS. The components shown in Figure 13 are sorted in Table 7 to distinguish AWORe components from the components already existed at the test field.

Table 7. AWORe components

AWORe components	Other components
Primary PC	Boson PC
Secondary PC	Test field NAS
AWORe NAS	Gigabit Ethernet switch 1
Gigabit Ethernet switch 2	Sensor network
Network cameras	Port server
High-speed camera	
Microphone	

Primary PC runs the AWORe software and also hosts the webserver for the web UI. The software development process is presented in Section 3.3. AWORe network storage array (NAS) is used to store all gathered data (Section 3.2.5). Gigabit Ethernet switch 2 is needed to connect network cameras and the HSC to Vaisala network. Network cameras are used to record occurring weather conditions and are presented in Section 3.2.1. AWORe uses microphone to continuously record audio to assists in distinguishing between frozen and liquid hydrometeors (Section 3.2.3). The HSC is used to capture individual hydrometeors, allowing closer examination of individual hydrometeors. The HSC setup is presented in Section 3.2.2.

3.2.1 Network cameras

AWORe is required to use two network cameras. The primary network camera is used to display a contrast plate continuously, whereas the secondary camera pans sensors at the test field. Network cameras were chosen for AWORe considering the requirements. Cameras are both similar and their type is AXIS Q6045-E MK II. Specifications of the camera compared to the requirements are shown in Table 8.

Table 8. AXIS Q6045-E specifications compared to the requirements. [45]

Requirements		AXIS Q6045-E Specifications
Operational temperature	-40 ... +50 °C	-50 ... +50 °C
IP-classification	IP 66	IP 66
Resolution	1920 x 1080 px	1920 x 1080 px
Frame rate	25 fps	25 fps
Optical zoom	20 x	32 x

As presented in Table 8, the camera fulfills all the requirements. The camera is able to capture video with 1920 x 1080 px resolution with 25 fps. The camera has 32 x optical zoom, hence it is able to display sensors which are not in the vicinity of the camera. Its operational temperature range is wider than required and also the IP classification is sufficient. However, the power supply of the camera, AXIS T8134 Midspan 60 W, has specified operational temperature range from -10 to +45 °C [46]. Therefore, the power supplies must be installed inside a heated enclosure to ensure the functionality of the power supply at -40 °C temperature.

The primary camera is used to capture close-up video of precipitations. Thus, it requires a contrast plate to enhance observation of precipitations. The contrast plate is required to be size of 660 x 660 mm, heated and illuminated by two LED lights. The plate is required to have matte black surface, as it has been found to be the best background for recording of precipitations [2]. It is also required to have markings to assist in hydrometeor terminal velocity and size estimation, as illustrated in Section 2.3.2. The markings on the contrast plate were designed according to [2]. The drawing of the plate is presented in Figure 14.

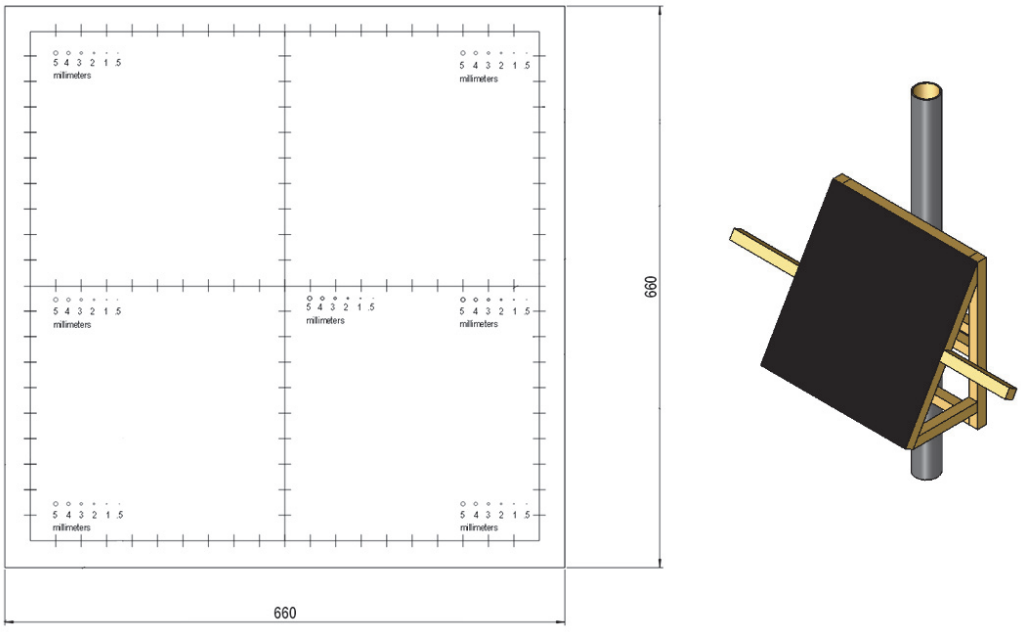

Figure 14. The contrast plate and the installation frame.

The contrast plate is fixed to the designed frame presented in Figure 14 and the installation height of the plate is 1.3 m. The installation height is measured from the center line of the contrast plate. Two 3W LED lights are used to illuminate the contrast plate. The lights are installed on the left and right side of the plate to achieve narrow light beam on the center line of the plate.

Narrow light beam was found during the development process to enhance the detection of hydrometeors. In addition, a collector plate is required to be installed below the contrast plate to collect hydrometeors. The purpose of the collector plate is to assist in detection of solid hydrometeors, as they bounce from the surface. The heating of the contrast and collector plates is performed by three heating foils. The foils are attached on the backside of the plate. The heating foils have total power of 220 W, requiring power supply of 220 W and temperature dependent relay to control the heating.

The power supply used is Chinfa DRW240 and the relay is ENSTO ECO 16FD. The power supply has power of 240 W. The relay uses one temperature sensor to measure temperature and has threshold temperature range from 0 to +5 °C. Since heating is necessary only at temperatures close to 0 °C, the range is adequate. The relay is set to +5 °C position activating the heating, as temperature decreases below +5 °C. The heater power supply and power supplies of the network cameras require an enclosure, as they have no IP 66 classification. The power supplies of the network cameras also require heating, as described earlier in this section. Therefore, two separate enclosures are used to cover the components. The enclosure containing the power supplies of the network cameras is illustrated in Figure 15.

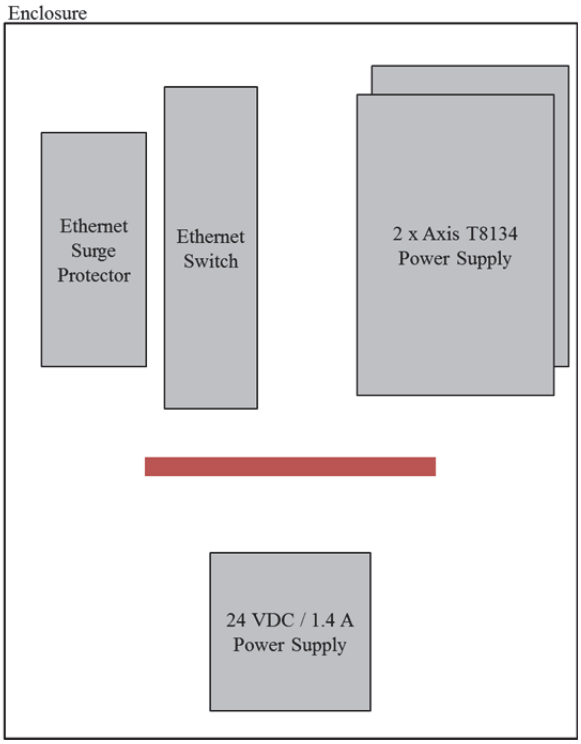

Figure 15. Enclosure for the power supplies of the network cameras

As can be seen from Figure 15, the enclosure contains also the gigabit Ethernet switch, power supply for the switch and a surge protector. The surge protector is required to protect the switch from over voltages occurring, e.g., due to lightning. The power supplies are installed to a stack, so that there is 1 cm space between them. The enclosure is heated by one 60 W foil, which is illustrated as a red element (Figure 15). The relay and the heating power supply are installed inside a separate enclosure.

The network cameras are installed to the test field to a pole mast. The primary camera is required to be installed perpendicularly to the contrast plate, to avoid errors in terminal velocity estimation due to an oblique arrangement. The installation height of the primary camera must be 2.8 m, as the height of the pole mast is 3 m and the secondary camera must be installed above the primary camera. The installation height of the contrast plate is required to be 1.3 m.

Since the slant distance is required to be 3 m and the installation height of the camera and the contrast plate are known, the distance between the camera and the contrast plate can be calculated using Pythagoras's theorem as follows:

$$b = \sqrt{a^2 - c^2} = \sqrt{1.5^2 - 3^2} = 2.6 \tag{16}$$

The installation height of the contrast plate is subtracted from the installation height of the camera to achieve the length of the a-side in Equation 16. The installation angle of the contrast plate can be calculated such that

$$\alpha = \sin^{-1}\left(\frac{a}{c}\right) = 29.9\,° \tag{17}$$

As shown in Equation 17, the installation angle is approximately 30 °. The primary camera and contrast plate arrangement is illustrated in Figure 16.

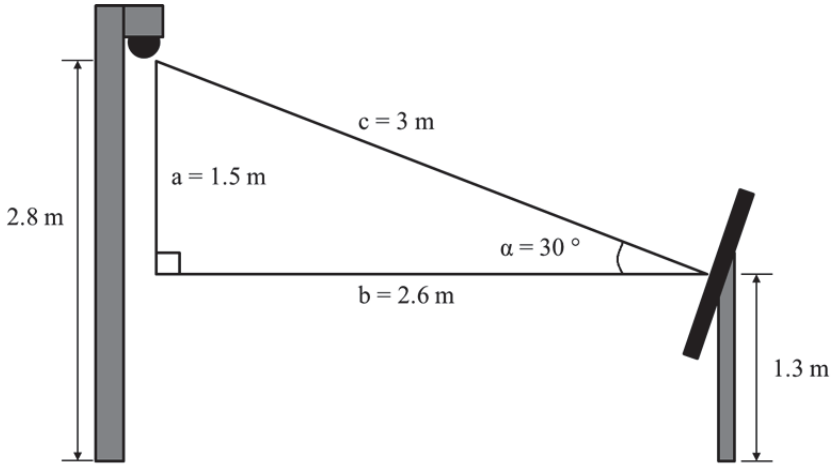

Figure 16. Primary camera and contrast plate arrangement

The primary camera and the contrast plate are installed as illustrated in Figure 16. Thereby, all requirements related to the installation of the primary camera and contrast plate are met. The secondary camera is installed above the primary camera when its installation height is approximately 3 m. The installation height allows the secondary camera to display all necessary sensors at the test field. The pole mast with the cameras installed as well as the contrast plate, the HSC setup and the audio recording setup are presented in Figure 17.

Figure 17. The network cameras and target plate installed

The network cameras are required to display various views. The primary camera displays three different views to provide good general view of the occurring weather, as shown in Figure 18.

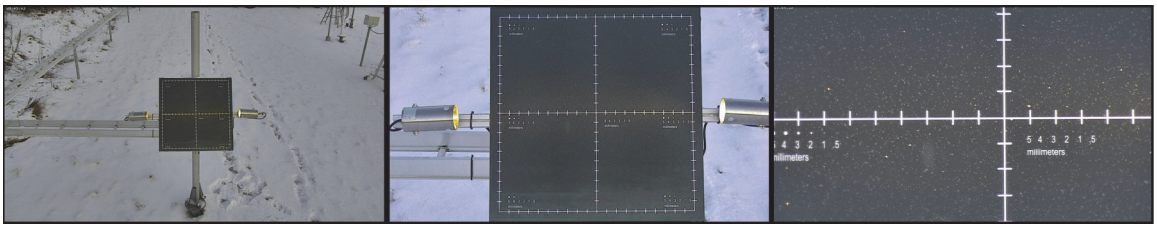

Figure 18. Primary camera views

The camera stays 15 seconds at each view and then the camera automatically changes the view. In contrast to the primary camera, the secondary camera pans sensors at the test field and displays open field views. The secondary camera displays one view at a time for 15 seconds as well. The secondary camera is used primarily to detect any water, snow or ice accumulation on the sensors and to see, the general view of the occurring weather. The open field view is also used to detect any occurring obscuration. The views can be adjusted using the camera software. Example views of the secondary camera are presented in Figure 19.

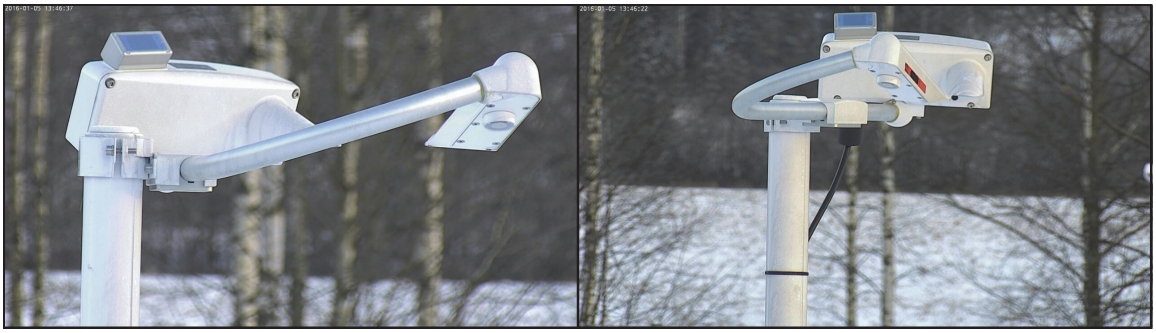

Figure 19. Example views of the secondary camera

The secondary camera is adjusted to display 7 different views during one round. One full round lasts 1 minute and 45 seconds. Camera settings are configured almost similarly for both cameras. The only difference is that the primary camera has an IR cut filter on. The IR cut filter prevents camera from seeing any infrared light. The primary camera must have the filter on, since it displays the illuminated contrast plate. Conversely, the secondary camera must not use the filter to enhance its night vision. The secondary camera displays sensors at the test field, which are not illuminated and thus, the enhanced night vision is required. The activation of the IR cut filter is the only difference between network camera settings. All primary camera settings are shown in Figure 20.

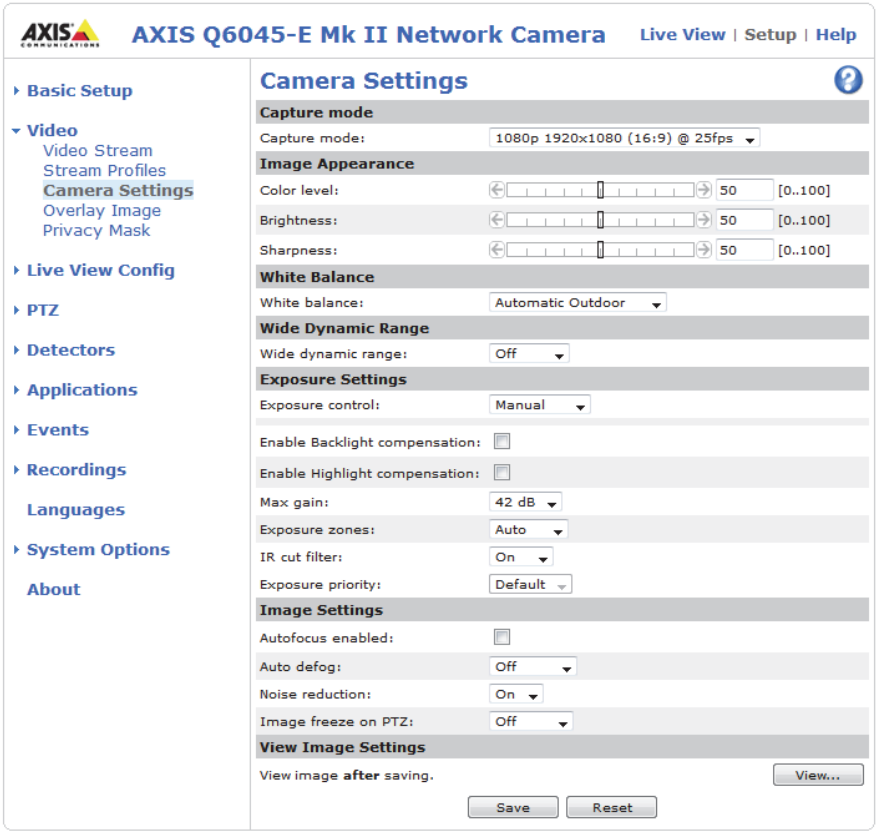

Figure 20. Primary camera settings

3.2.2 High-speed camera

A HSC is required for AWORe, since the network cameras are not able to clearly capture individual droplets. Recording of fast objects, such as hydrometeors, requires certain attributes from the camera and light source, as described in Section 2.3. It is stated in the requirements that the maximum allowed motion blur is 0.5 mm. Required exposure times to capture hydrometeors with terminal velocity of 10 m/s were presented in Table 5. According to Table 5, shortest exposure time needed is approximately 44 us. The height of the FOV to be used is 30 mm and the required resolution is 640 x 480 px. Consequently, the minimum frame rate can be estimated using Equations 12 and 14 as follows:

$$t_{pass} = \frac{0.03\ \text{m}}{10\ \text{m/s}} = 3\ \text{ms}$$

$$fps_{min} = \frac{2}{3\ \text{ms}} = 667\ \text{frame/s}$$

Presented values as well as interfaces and price were considered when the HSC was chosen for AWORe. The chosen HSC is Basler Ace ACA640-750uc. It has frame rate of 750 fps with 640 x 480 px resolution and shutter speed of 1/16949, which allows 59 us exposure time. It was calculated using Equations 12, 13 and 14 that the HSC is able to capture two images of hydrometeors that have a terminal velocity of 10 m/s, as they fall through the FOV. The HSC is also relatively inexpensive.

The HSC requires a PC for video recording and for storing data. It also requires software for automatic video recording. Consequently, video acquisition software was designed for the HSC. The software is developed using LV and Vision acquisition software (National Instruments), as presented in Section 3.3.3.

Since the minimum exposure time of the chosen HSC is 59 us, it is unable to clearly capture hydrometeors with terminal velocity of 10 m/s. According to Table 5, the HSC is able to clearly capture raindrops smaller than 4 mm and hails smaller than 5 mm. Since the raindrops are typically smaller than 4 mm in Finland (Figure 6), the HSC is able to capture most of the occurring rain droplets. Considering this and the price gap between the chosen HSC and the HSCs with significantly faster shutter speeds, the chosen HSC was reasonable choice for AWORe.

In selection of an objective for the HSC, DoF and focal length were considered. Required focal length depends on the distance between camera and the contrast plate, which should be at least 300 mm to avoid lens contamination by splashed water. The objective chosen for the HSC is Fujifilm Fujinon HF35SA-1, which has focal length of 35 mm and adjustable aperture from f/1.4 to f/22. The required distance between the HSC and the contrast plate to achieve the FOV with height of 30 mm using the objective can be calculated as follows [42]:

$$L = \frac{Y \times F}{Y'} = \frac{30\ \text{mm} \times 35\ \text{mm}}{2.7\ \text{mm}} = 389\ \text{mm} \tag{18}$$

In Equation 18, L is the distance between the camera and the object, Y is the height of the FOV, F is the focal length and Y’ is a vertical size parameter defined in the datasheet of the objective [42]. It is assumed in this thesis that sufficient DoF would be 30 - 50 mm. The target DoF is set to 40 mm and can be calculated using Equations 9 and 10. Calculated values are shown in Table 9.

Table 9. DoFs with various aperture sizes.

δ [mm]	f	L [mm]	F [mm]	Tr [mm]	Tf [mm]	DoF [mm]
0.03	1.4	369	35	4.7	4.6	9.3
0.03	1.4	369	35	4.7	4.6	9.3
0.03	2.8	369	35	9.6	9.1	18.7
0.03	4	369	35	13.8	12.9	26.7
0.03	5.6	369	35	19.7	17.8	37.4
0.03	8	369	35	28.8	24.9	53.6
0.03	11	369	35	40.7	33.4	74.1
0.03	16	369	35	62.4	46.6	109.0
0.03	22	369	35	91.6	61.2	152.8

In order to exploit the whole DoF, the contrast plate should be installed to the far sharp point. When DoF of 40 mm is used, the distance between objective and the far sharp point is approximately 389 mm. Therefore, that value is used in Table 9. As can be seen from Table 9, f-number of 5.6 should be used in order to achieve the DoF close to 40 mm. Corresponding EV seen in Figure 11 is approximately 20. Consequently, the required illuminance is much more than 100 000 lx. Since the approximated illuminance to achieve sufficient light conditions is so high, the f-number was decided to be decreased by one stop. By using f-number of 4, the EV is approximately 19.

A light source for the HSC was chosen considering required illuminance as well as specified operational conditions and availability of the light source. The chosen light source is Advanced Illumination RL169 Ultra Bright™. The maximum illuminance generated by the light at 300 mm distance is 67 000 lx. The illuminance corresponds to EV higher than 17, which is smaller than the calculated EV. However, availability of more efficient light sources is weak and also prices of such light sources would have been too high. Nevertheless, the light source was first tested in the laboratory environment and was found to be sufficient for the HSC.

The light source requires a 24 VDC / 2 A power supply. The light has IP 65 classification and an operational temperature range of 0 … +60 °C. Due to the insufficient temperature range, a heater must be used to keep the light source within the specified temperature range. The light requires also a heated hood to prevent water, snow or ice accumulation on its surface. Any accumulation weakens the produced illuminance.

The HSC and the objective require an enclosure to withstand outdoor conditions. The enclosure must be at least IP 66 classified and compact to ease its installation. AutoVimation Salamander enclosure was chosen, since it has IP 67 classification and is very compact. It also has installation kit for Basler Ace cameras easing the installation of the HSC inside the enclosure.

Recording of individual hydrometeors requires also a contrast plate. The contrast plate designed for primary camera has a matte black surface. However, it was found that the lighter surface is better for HSC use. Consequently, the contrast plate designed for the HSC has a white surface with matte black markings. The drawing of the designed plate is shown in Figure 21.

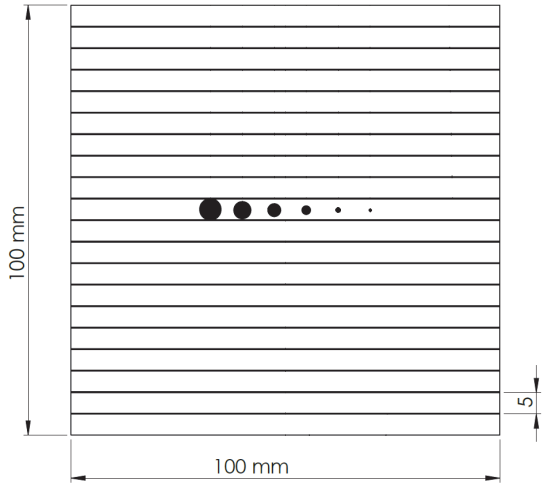

Figure 21. The designed contrast plate for the HSC

The HSC contrast plate has horizontal lines with the space of 5 mm and six differently sized dots in the middle. The dot sizes are: 0.5, 1, 2, 3, 4 and 5 mm. The lines and dots can be used in the terminal velocity and size estimation of hydrometeors, utilizing methods presented Section 2.3.2. The contrast plate is installed perpendicularly to the HSC, as presented in Figure 22.

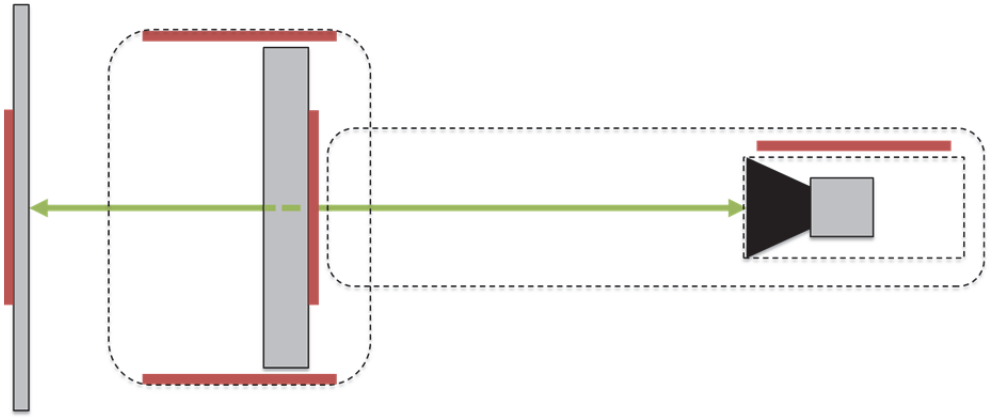

Figure 22. The plan view of the HSC-setup

The HSC displays the contrast plate through the hole of the light source. The diameter of the hole is 66 mm, which limits the FOV. The maximum FOV depends on the distance between the HSC and the light source as well as the distance between the camera and the contrast plate.

The HSC is installed inside AutoVimation Salamander enclosure, as described earlier in this section. The enclosure is installed inside a pipe to avoid contamination of the enclosure glass. The pipe extends below the hood of the light source, as illustrated in Figure 22. All parts of the HSC-setup are heated and the red elements shown in Figure 22 illustrate the used heating foils. The power consumption of each foil is 66 W. Thus, the total power consumption is 330 W. Two 240 W power supplies are used for the heating. The heating is controlled by two temperature dependent relays.

An industrial PC is required to control the HSC, since the HSC is unable to independently record and store videos. The PC utilized to control the HSC is Advantech ARK-1550-S9A1E. It has Intel® 4th generation Core i5 processor and 8 GB DDR3L RAM. The PC has operation temperature range of 0 … +40 °C. The PC is essentially used in video recording, but it also records audio, as described in Section 3.2.3. The recording is controlled by the developed software presented in Section 3.3.3. The PC and the heating power supplies are installed inside an enclosure illustrated in Figure 23.

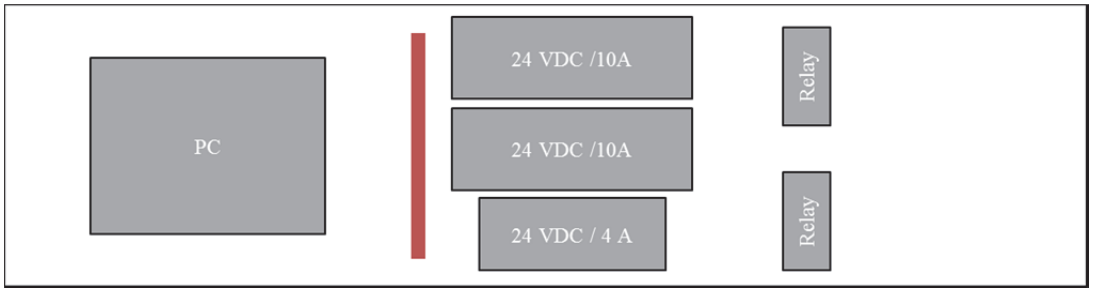

Figure 23. The HSC terminal box

The enclosure is also heated by one 66 W heating foil to keep the temperature above 0 °C. The relays illustrated in Figure 23 are set to active heating when temperature decreases below +5 °C. The enclosure is installed to the same pole mast with the network cameras (Figure 17).

3.2.3 Audio recording setup

AWORe is required to continuously record audio to assists in distinguishing between frozen and liquid hydrometeors. The network cameras presented in Section 3.2.1 do not have audio input. Therefore, an external microphone is required. AXIS T8351 microphone was chosen for AWORe since it is from the same manufacturer as the network cameras. The microphone has IP 66 classification and operating temperature range from -20 to +60 °C, allowing outdoor installation. [47]

The microphone is installed inside a metallic dome, which is attached to the same pole mast with the network cameras (Figure 17). The metallic dome is used to generate recognizable sound when liquid or frozen precipitations hit on its surface. The dome is heated by one 66 W foil to avoid accumulation of ice and snow on its surface. The heating also heats the microphone, when the functionality of the microphone is ensured at the -40 C temperature, as required (Section 3.1). The audio recording setup is illustrated in Figure 24.

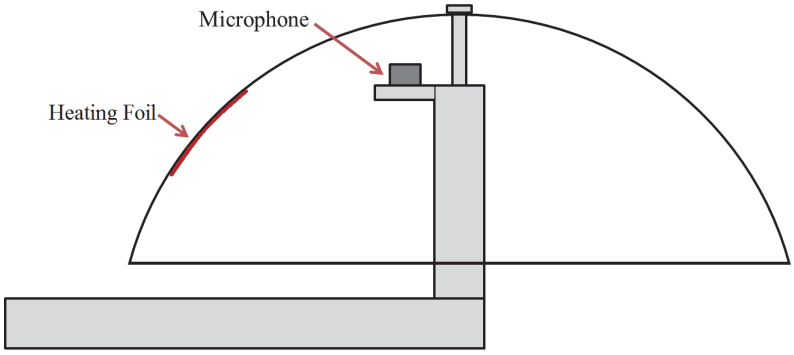

Figure 24. Audio recording setup

The microphone is connected directly to the audio input of the HSC PC. Designed audio recording software is used in audio recording and is presented in Section 3.3.4. The heating power supply used for the HSC heating is also used to power the used heating foil.

3.2.4 Sensor network

AWORe is required to measure various weather parameters. In addition, it is required to detect changes in occurring weather and report them. AWORe was designed to utilize comprehensive assortment of weather instruments to fulfill these requirements. AWORe has two different purposes for the weather instruments. A sensor either provides real-time weather data to support precipitation type classification or is used as a weather event trigger.

Sensors providing only real time weather data are hard-coded to the AWORe software new sensors cannot be added later without performing changes to the developed software. These sensors and acquired parameters are described in Table 10.

Table 10. Weather instruments used by AWORe.

Instrument	**Parameters**
Vaisala HMP155	Temperature, relative humidity
Vaisala PTB330	Air pressure
Vaisala WMT700	Wind speed, wind direction
Vaisala CL31	Cloud height and amount of two layers
Vaisala FD12P	Visibility (MOR)
OTT Pluvio²	Precipitation intensity and accumulation
OTT Parsivel	NWS code, precipitation accumulation
Thies Clima Laser Precipitation Monitor	METAR, precipitation accumulation

The parameters presented in Table 10 are fundamental weather parameters that provide essential information for precipitation type identification. AWORe uses Vaisala HMP155 for measuring temperature and relative humidity. HMP155 uses the Vaisala HUMICAP® technology in relative humidity measurements. HMP155 has wide temperature and relative humidity measurement ranges. Temperature range is from -80 to +60 °C and relative humidity range is from 0 to 100 %. Due to the wide measurement range and good accuracy, HMP155 is suitable sensor for AWORe. [48] [49]

AWORe uses Vaisala PTB330 digital barometer for measuring air pressure. PTB330 uses Vaisala BAROCAP® technology. PTB330 Class A measurement range is from 500 hPa to 1100 hPa and temperature range from -40 to +60 °C. Class A PTB330 accuracy is ±0.15 hPa. [50]

Wind speed and direction are measured by Vaisala WMT700, which utilizes the Vaisala WINDCAP® technology. The sensor has three transducers, which all transmit ultrasound to other two transducers and correspondingly receive ultrasound from the other two transducers. Wind speed and direction are calculated from the ultrasound time of flight, which is measured from three distinct paths.

AWORe uses Vaisala CL31 to measure sky condition. Sky condition is description for the height and amount of occurring cloud layers. CL31 measures the height and amount of five cloud layers. However, AWORe uses only measurement data of the lowest two cloud layers. Sky condition measurement utilizes backscattering principle.

The measurement is performed by transmitting short laser pulses and receiving backscattering signal from the clouds. The cloud height is calculated from the time difference between the transmission and receiving. [51]

AWORe utilizes Vaisala FD12P to measure visibility in MOR. Visibility is determined measuring scattering coefficient, as described in Section 2.2.1. FD12P is also able to measure present weather utilizing forward scatter measurement, temperature measurement and capacitive precipitation measurement. [52]

OTT Pluvio² weighing rain gauge is used to measure precipitation intensity and accumulation. Pluvio is able to measure intensity and accumulation of rain, snow and hail. Weighing principle is accurate precipitation accumulation measurement method. Accuracy in precipitation accumulation measurement is ±0.05 mm and ±0.1 mm/min in intensity measurement. Disadvantage of the sensor compared to PWSs is its limited precipitation type range. [53]

OTT Parsivel is a laser-based disdrometer. Parsivel is used to determine present weather parameters. The used measurement technology differs from forward scatter measurement. The sensor detects signal changes in intensity of received light. The difference to forward-scatter measurement is that as a hydrometeor falls through the laser beam, fast amplitude drop is detected in the signal. Precipitation type is determined by analyzing the amplitude and duration of the peak. The amplitude determines the size of the hydrometeor, whereas the duration determines the terminal velocity of the hydrometeor. AWORe acquires precipitation type and accumulation information from the sensor. [54]

Thies Clima Laser Disdrometer is also a PWS that utilizes same measurement principle as Parsivel. Thies Clima Laser Disdrometer reports precipitation type only in METAR, unlike the other PWSs used which are reporting both, METAR and NWS code. Consequently, AWORe acquires precipitation accumulation information and METAR from the sensor. Although METAR and NWS code are different, as described in Section 2.1.1, they contain nearly the same information and are thus, comparable.

In addition to the sensors presented, AWORe has capability to use 10 manually chosen event trigger sensors. Every time a trigger sensor detects change in current weather, AWORe generates an event. Each event is added to the daily report, as described in Section 3.3. The weather events are detected by continuously reading trigger parameters. The trigger parameters are parameters that trigger sensors natively report.

The parameters are selected before system start-up and can be re-selected on software front panel, as described in Section 3.3.2. The default event trigger sensors and parameters are shown in Table 11.

Table 11. The default event trigger sensors.

Trigger no.	Sensor type	Trigger parameter
1	Vaisala PWD52	NWS code
2	Vaisala PWD52	NWS code
3	Vaisala PWD52	NWS code
4	Vaisala PWD52	NWS code
5	Vaisala PWD52	NWS code
6	Vaisala PWD52	NWS code
7	Vaisala PWD22	NWS code
8	Vaisala PWD52 (External temperature measurement)	NWS code
9	Vaisala FD12P	NWS code
10	OTT Parsivel	NWS code

It can be seen from Table 11 that most of the event trigger sensors are Vaisala PWDs. PWDs utilize forward scatter principle, whereas OTT Parsivel and Thies Clima Laser Disdrometer utilize different optical measurement principle, as presented earlier in this section. Thus, AWORe uses PWSs that utilize two different optical measurement principles, as required (Section 3.1).

Additionally, AWORe utilizes Vaisala FD12P and OTT Parsivel PWSs as event trigger sensors. In total, AWORe uses five different types of PWSs as event trigger sensors, allowing it to detect most of the precipitation events. Each PWS type uses different algorithm, achieving increased probability to detect all precipitation events. However, PWSs are unable to distinguish all precipitation types, as described in Section 2.2.

In order to enhance detectability of precipitation events, a web UI where users may submit observations is developed in this thesis (Section 3.3.5). The web UI is primarily designed to assists AWORe for detecting the events that the trigger sensors are not necessarily able to recognize. Events detected by the event trigger sensors are also used to control the HSC, as described in Section 3.3.3.

Measurement data acquisition from the sensors is performed using a distinct PC running Vaisala Boson. Vaisala Boson is data logging and simulation software that is used only internally in Vaisala. Measurement data logging process is shown in Figure 25.

Figure 25. Measurement data acquisition process

Individual sensors are connected directly to the port server via RS232 or RS485 line. The purpose of the port server is to serve as serial line to Ethernet converter. It also defines IP address for each sensor. The data acquisition process functions so that Vaisala Boson polls a sensor and the sensor responds by sending a message back to Boson. Some of the sensors are configured to send an automatic message in specified time interval. In that case, Boson does not need to poll the sensor.

Boson creates an individual log file for each sensor. The log files are updated every time Boson receives a new message from sensors. AWORe software continuously reads log files, receiving real-time information from the sensors.

3.2.5 Data storage

Since AWORe continuously records video and audio, enormous amount of data is gathered. Consequently, data storage device with large capacity is required. It is estimated that the daily amount of data is close to 200 GB. The estimation is based on the size approximation of network camera recordings and HSC recordings. AWORe is required to have capability to store all data for 30 days. Thus, the total amount of gathered data in 30 days is estimated such that:

$$\text{Total amount of data} = 30 \text{ days} \times 200 \text{ GB / day} = 6 \text{ TB} \quad (19)$$

As shown in Equation 19, the estimated data amount gathered in 30 days is 6 TB. Therefore, Lenovo EMC™ px4-400r NAS with the capacity of 8 TB was chosen for AWORe.

The NAS utilizes Redundant Array of Independent Disks (RAID). RAID essentially combines smaller storages into a one larger storage. RAID has several different levels and each level form the NAS storage differently. For example, RAID 0 only combines smaller storages into a one larger storage, whereas RAID 5 distributes parity information to all individual hard disks used. [55]

RAID 5 has higher redundancy than RAID 0, since stored data is not lost if a single hard disk failures. However, RAID 5 decreases the available storage space significantly. For example, RAID 5 would limit the real storage space to approximately 2 TB if 8 TB storage device that consists of four single 2 TB hard drives would be used. Therefore, AWORe NAS is configured to use RAID 0 to have a capability to store data of 30 days. Using RAID 0 the real storage space is 7.59 TB. Thus, the maximum amount of daily-data can be calculated by re-forming Equation 19 as follows:

$$\text{daily-data}_{\max} = \frac{\text{Total amount of data}}{\text{days}} = \frac{7590\ \text{GB}}{30} = 253\ \text{GB} \tag{20}$$

As shown in Equation 20, AWORe is able to store data of 30 days if the daily-data amount is less than 253 GB. In order to enhance the redundancy of the data storage, an external storage device could be used. External storage devices are relatively cheap and small sized. Those could also be used to archive old data.

3.3 Software development

AWORe requires software to connect all individual components to function as a system. AWORe software was developed using LV. LV is graphical programming environment, which uses graphical G-language. LV-based software are built using virtual instruments (VI). A main VI is the top level of the software and contains typically numerous sub VIs. This architecture is necessary to keep the code readable. The front panel of the main VI is used to configure the software. The front panel of the AWORe software is presented in Section 3.3.2. The AWORe software does not directly interact with all parts of AWORe. Interaction between the software and individual components is presented in Figure 26.

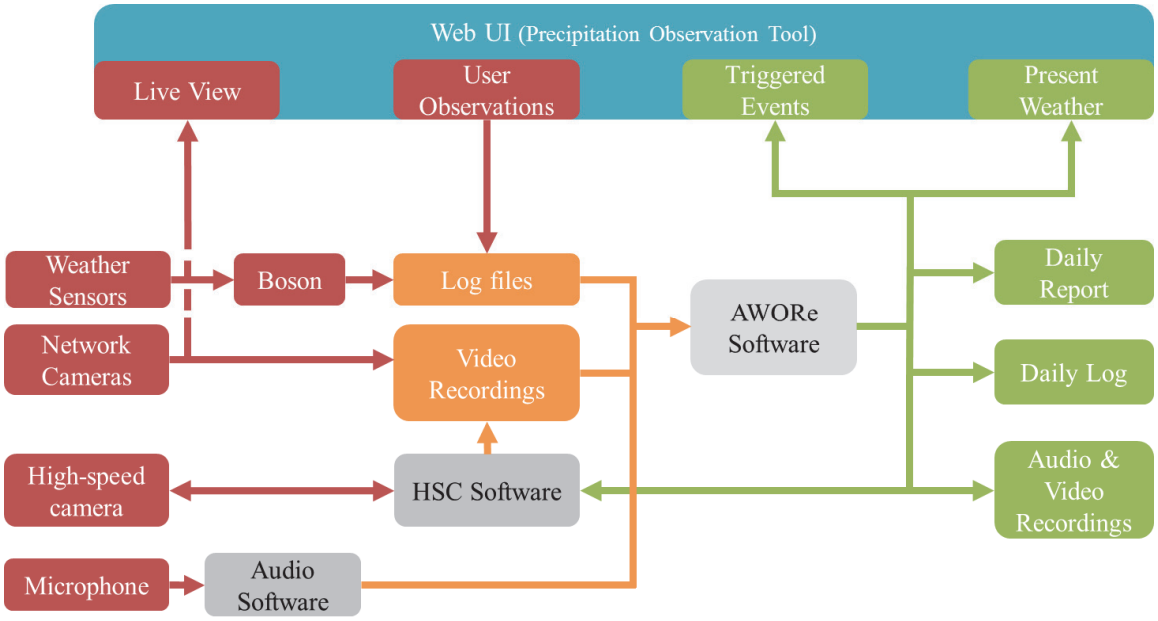

Figure 26. AWORe software interaction with the individual components

As can be seen from Figure 26, the individual parts of AWORe perform several functions without interaction with the software. In addition to the AWORe software, two distinct software are designed for high-speed video and audio recording (Sections 3.3.3 and 3.3.4). The AWORe software has four main tasks, which it must perform. The tasks are listed below:

1. Read data from log files.
2. Detect event changes and process measurement data.
3. Continuously update the web UI.
4. Generate the daily report.

Flowchart description of the AWORe software is presented in Figure 27.

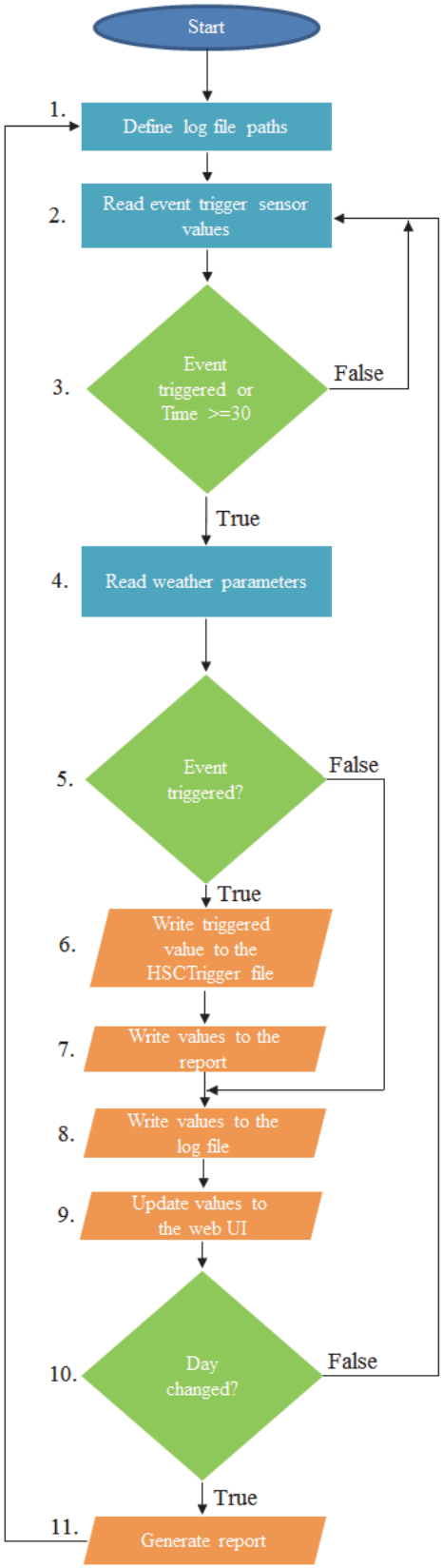

Figure 27. The flowchart of the AWORe software

The flowchart is top level description of the software and presents only the top level phases. As can be seen from Figure 27, after the software is started the first step is to define the log file paths. The second step is to read current values from the event triggers. As the latest values are read, the software compares the values to the conditions defined on the front panel. If any of the sensors has triggered an event or 30 seconds has elapsed, software proceeds to the fourth step.

The fourth step is to read latest values from the other sensors. The fifth step is to decide which log files to be updated. If an event is triggered, the value from the event trigger sensor that has triggered the event is written to the HSC trigger file. Additionally, all values from the sensors are written to the report file. If no event is triggered, the software proceeds straight to the 8th step without adding new values to the HSC trigger and report files. In the seventh step, the software writes latest values to the daily log file. In the next step, latest values are updated to the web UI.

The final step is to check whether the day has changed. The software stays in a loop repeating the steps 2-10 until the day changes. As the day changes, software generates the daily report and stores all log files to the NAS. Before this step, all the log files are in the hard drive of AWORe PC or in the test field NAS. When these actions are done the software proceeds to step 2 and defines the log paths for the new day and moves again into the loop.

As described earlier, the first task is to read data from the log files. The log files are stored on the test field NAS and log file paths are changed daily. Therefore, the log file path must be defined every day. A format of the log files is defined in Boson. Boson is configured to use the following format:

Xymmdd00.dat

The first character above is defined for each sensor individually. The first character varies and is used to distinguish between identical sensors. Next five characters designate the current date. The last two characters are additional and not all sensor filenames include them. The paths are defined by formatting the current date to the correct format. After sorting the date, the beginning and the end of the path are concatenated to a string. The beginning of the path is defined on the front panel of the software when AWORe is configured (Figure 30). The defined log paths are used by Event trigger VI to read data from the log files. Functionality of the Event trigger VI is described in Figure 28.

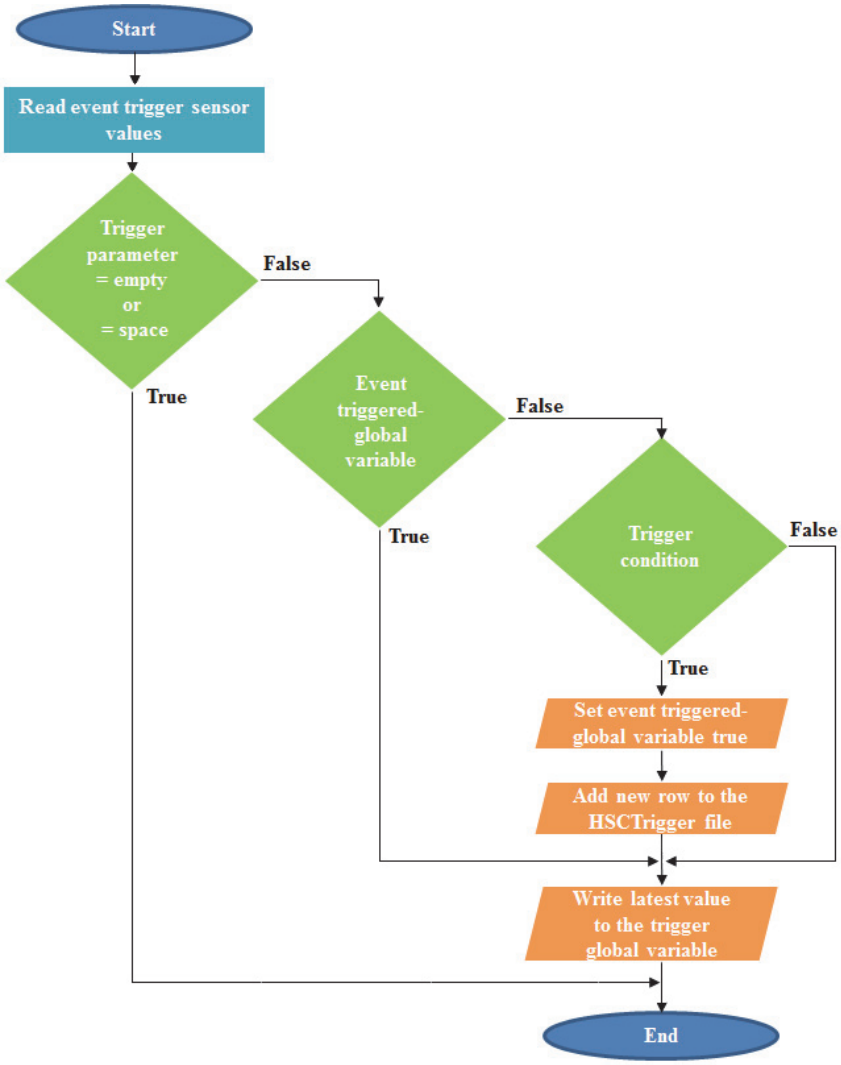

Figure 28. The flowchart of the Event trigger VI

The Event trigger VI first reads the value of the trigger parameter from the log file. As the value is read, the VI compares the value to empty and space strings. This comparison is performed to detect any errors occurred during data reading. The empty string or the string containing only space may occur, if the log file is read at the same time as the log file is updated. If no errors are detected, software proceeds to the next comparison where state of the event trigger-global variable is checked. If the state is true, the VI writes the value to the trigger global variable and ends the VI. If the state is false, the VI proceeds to the next comparison where the value is compared to the trigger condition defined on the front panel (Figure 31). All available trigger conditions are shown in Table 12.

Table 12. Available event trigger conditions.

x = Latest value y = Previous value	**x**	**=**	**y**
	x	**!=**	**y**
	x	**<**	**y**
	x	**>**	**y**
N = Numeric value	**x**	**=**	**N**
	x	**!=**	**N**
	x	**<**	**N**
	x	**>**	**N**
S = String	**x**	**=**	**S**
	x	**!=**	**S**

The comparison can be performed, e.g., between the two latest values which is the default case. For instance, when PWD52 is set to operate as a trigger sensor and NWS code is set to a trigger parameter, PWD52 triggers an event every time reported NWS code changes. In addition, the latest value can be compared to a numeric value or a string defined on the front panel. These are useful when only specific events are under interest. For example, if only hail events are wanted to be triggered, the string variable can be set to "A" and comparison condition can be set to x = S. Then the software triggers an event only when the trigger sensor is reporting "A". Correspondingly, if weak visibility conditions would be under interest, threshold visibility could be defined by using a numeric value.

If the trigger condition is true, the software sets the triggered event-global variable true and writes the value to the HSC trigger file. This file is used by the HSC software to detect triggered events. The actual HSC triggering is performed by the HSC software (Section 3.3.3).

As the HSC trigger file is updated, the VI writes the latest value to the trigger global variable. Each event trigger sensor consecutively executes the Event trigger VI. Executing the VI 10 times lasts approximately 2 seconds. Hence, the software is theoretically able to detect any changes in the occurring weather with 2 seconds delay. However, sensors are typically reporting with 30 seconds interval thus, the real delay is approximately 30 seconds. The sensors are not synchronized with each other i.e., they are not reporting at the same time. Therefore, it is necessary to continuously read the latest values. Each trigger sensor has own trigger global variable where they store the latest values. These global variables are used to compose the report. The report formation and its content are described in Section 3.3.1.

3.3.1 Daily report

AWORe is required to daily generate a report that contains all triggered events and sensor readings at the time of each triggered event. The report is generated by the AWORe software every day as a day changes. The daily report assists observers by pointing all the interesting events detected by the event trigger sensors during a day. Thus, the observers are not necessarily required to view 24 hours lasting video recordings. The observers may only view recordings at the time of the triggered events. That makes the work of observers remarkably easier. However, if only recordings at the time of triggered events are viewed some events may be missed, since the event trigger sensors are unable to detect all precipitations.

The global variables where all the latest values are stored are used to compose the report by writing all the values to an array (Section 3.3). The array is formed using build array function, as shown in Figure 29.

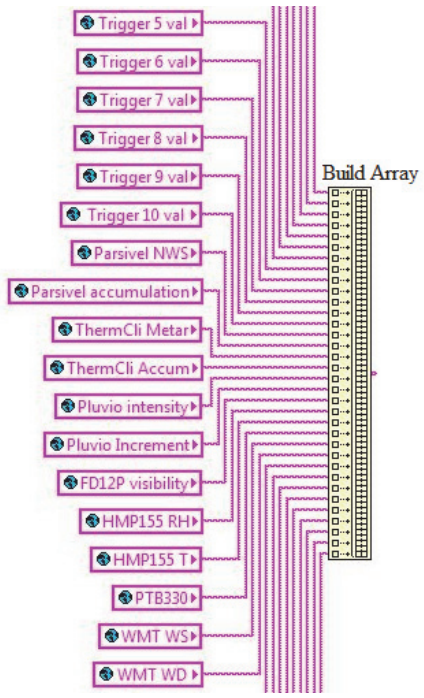

Figure 29. Writing latest sensor values to the report

The built array is appended to the report file using the Write to spreadsheet file VI. Every time an event is triggered a new array is added to the report file. The report file is stored in the AWORe PC hard drive until the day changes when the file is moved to permanent position and is then available for users.

The users may follow the weather conditions during the day from the web UI (Section 3.3.5). In this section, the complete report is presented in three parts and the first part is shown in Table 13.

Table 13. The first part of the daily report

		PWD	PWD	PWD	PWD	PWD	PWD	PWD	FD12P	Parsivel	Thies Clima
Time	Trig. No.	1	2	3	4	5	6	7	8	NWS Code	METAR
11:57:09	8	Clear	Light snow	Light snow	Light snow	Light snow	Light snow	Clear	Light snow	C	-SG
11:58:48	7	Clear	Light snow	Light snow	Light snow	Light snow	Light snow	Light snow	Light snow	C	-SN
11:59:02	1	Light snow	Light snow	Light snow	Light snow	Light snow	Light snow	Light snow	Light snow	C	-SN
11:59:13	8	Light snow	Light snow	Light snow	Light snow	Light snow	Light snow	Light snow	Light ice crystals	C	-SN
12:09:47	8	Light snow	Light snow	Light snow	Light snow	Light snow	Light snow	Light snow	Light snow grains	C	-SN
12:13:52	8	Light snow	Light snow	Light snow	Light snow	Light snow	Light snow	Light snow	Light snow	C	-SN
12:18:17	8	Light snow	Light snow	Light snow	Light snow	Light snow	Light snow	Light snow	Light snow grains	C	-SG
12:20:17	8	Light snow	Light snow	Light snow	Light snow	Light snow	Light snow	Light snow	Light ice crystals	C	-SG
12:27:48	4	Light snow	Light snow	Light snow	Light snow	Light snow	Light snow	Light snow	Light ice crystals	C	-SG
12:28:05	User	Light snow	Light snow	Light snow	Light snow	Light snow	Light snow	Clear	Light ice crystals	C	-SG
12:29:30	1	Clear	Light snow	Light snow	Light snow	Light snow	Light snow	Clear	Light ice crystals	C	-SG

The report is fundamentally a table that presents all the information acquired by AWORe at the time of each triggered event. The first part of the report shown in Table 13, presents triggered events within the presented time range. In addition, the first part of the report contains also readings from Parsivel and Thies Clima Disdrometer. However, these two PWSs are not functioning as event triggers. They are part of the sensor network and are measuring present weather.

The report indicates the sensor that has triggered an event at each point by a number. Since AWORe may use simultaneously at the most 10 event trigger sensors, the numbers are from 1 to 10. For example, the third event in Table 13 is triggered by the first PWD, when it has started to report light snow instead of clear. Although event trigger sensors are reporting NWS codes, the values are presented as precipitation types in the report (Table 13). The AWORe software converts NWS codes to precipitation types to ease the reading of the report. It can be seen from Table 13 that at the time of the third event all event triggers have reported the same precipitation.

Thies Clima Disdrometer also reported light snow, but Parsivel reported clear for the whole time range shown in Table 13. The weather data acquired by the sensors that are not event triggers is in the second part of the report presented in Table 14.

Table 14. The second part of the daily-report

Pluvio	Pluvio	FD12P	HMP155	HMP155	PTB330	WMT700	WMT700	CL31	CL31	CL31	CL31
mm/h	mm	m	%RH	°C	hPa	m/s	°	m	octas	m	octas
0	0.25	13388	78.4	-11.9	996.18	2.7	353	530	7	0	0
0	0.25	13472	78.4	-11.9	996.18	1.7	58.7	530	7	0	0
0	0.25	13489	78.4	-11.9	996.18	1.8	38.7	530	7	0	0
0	0.25	13631	78.4	-11.9	996.18	1.9	58.1	530	7	0	0
0	0.25	7485	78	-11.7	996.22	1.6	52.8	460	8	0	0
0	0.25	9232	78.3	-11.7	996.33	1.5	76.8	320	8	0	0
0	0.25	12607	78.3	-11.7	996.33	2.4	53.9	320	8	0	0
0	0.25	14358	78.6	-11.8	996.33	1.8	30.7	320	7	0	0
0	0.25	30326	77.9	-11.7	996.38	1.9	26.8	320	7	0	0
0	0.25	32312	77.7	-11.6	996.38	1.3	28.4	320	7	0	0
0	0.25	30447	77.4	-11.6	996.38	2.9	65.3	320	7	0	0

As can be seen from Table 14, the report contains all parameters described in Section 3.2.4. The reported parameters provide very comprehensive information about the current weather, assisting observers in precipitation identification. The third part of the report shown in Table 15 contains user observations and paths for both, audio and video recordings.

Table 15. The third part of the daily report

User Observation	User NWS code	User Note	Camera 1	Camera 2	HSC	Audio
			Path	Path	Path	Path
			Path	Path	Path	Path
			Path	Path	Path	Path
			Path	Path	Path	Path
			Path	Path	Path	Path
			Path	Path	Path	Path
			Path	Path	Path	Path
Light snow	S-		Path	Path	Path	Path
			Path	Path	Path	Path

It can be seen from Table 15 that one human observation is done within the time period in the report. The report presents the precipitation type determined by the observer and the corresponding NWS code. Additionally, the report contains the user note column where the observer may describe the precipitation more closely when necessary. The notes are written on the web UI when the observation is submitted. The web UI is presented in Section 3.3.5.

In addition to the daily report, AWORe generates also a daily log, which includes the same information than the report. The log contains sensor readings with one minute interval, providing weather data of the whole day.

3.3.2 Front panel

AWORe software has a graphical user interface (GUI) where the software is configured. The GUI is the front panel of the main VI. The front panel contains many configurable parameters, which are related to the event trigger sensors. The part of the front panel where event trigger sensor types and their log file path are defined is shown in Figure 30.

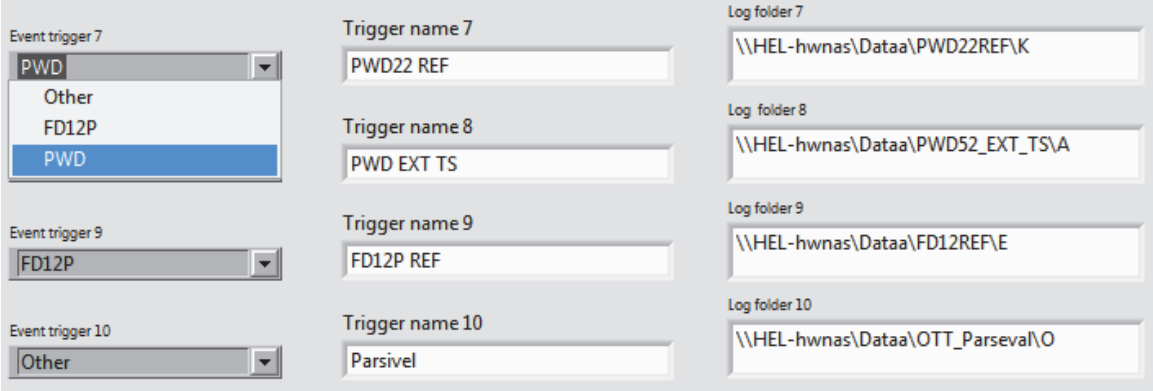

Figure 30. Event trigger sensor definitions on the front panel

The front panel has the three fields for each event trigger sensor. Each trigger sensor can be named to make the report easier to read. The trigger name is shown in report above the trigger number (Table 13). The log folder must be defined for each sensor so that the software may automatically build the log path, as described in Section 3.3. The drop-down menus contain two preset sensors and an option for manually adjustable sensor. If the option “other” is chosen, the fields shown in Figure 31 must be adjusted.

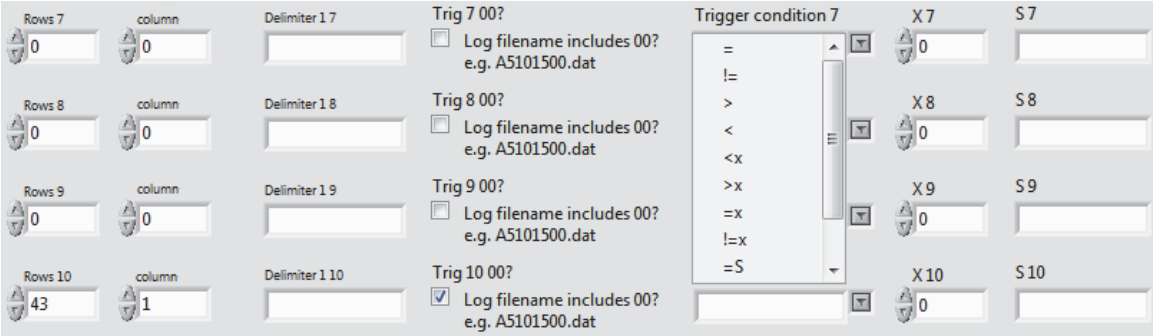

Figure 31. Event trigger sensor configuration

Since OTT Parsivel is used in AWORe as an event trigger sensor, the parameters shown in Figure 31 must be adjusted for it. As can be seen from Figure 31, the row and column parameters are defined. Additionally, the checkbox is checked, since the Parsivel log filename contains “00”. Parsivel uses the default trigger condition. If any other trigger condition would be used, it should have been defined on the drop-down menu shown in Figure 31.

3.3.3 High-speed camera software

Video recording software was developed for the HSC, to automatize high-speed video recording as well as to enable interaction between the AWORe software and the HSC. The recording software was developed using LV and NI Vision Acquisition Software. The recording software communicates with the HSC via USB3 Vision interface. As the software utilizes USB3 Vision interface, it is compatible with any USB3.0 camera supporting USB3 Vision interface. The recording software fundamentally performs two functions, which are:

- HSC triggering.
- Image acquisition from the HSC.

HSC triggering function is required, since the HSC cannot continuously record, due to the enormous amount of data the HSC generates. The HSC is triggered to record only when precipitation events occur. The main VI of the recording software is presented in Figure 32.

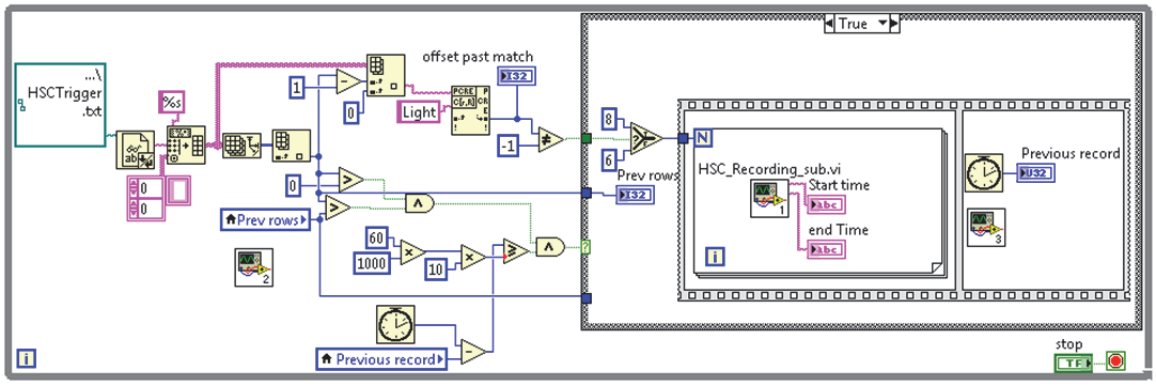

Figure 32. The main VI of the recording software

The presented VI continuously reads the HSC trigger log file where all triggered events are added by the AWORe software (Section 3.3). The VI detects increased row count of the log file.

As increased row count is detected, the VI compares current time to the time of a previous recording sequence. In order to start new recording, the time between two recording sequences must be greater or equal to 10 minutes. The delay between two recording sequences is required to limit the number of recordings.

The number of recordings within one recording sequence was designed to depend on the precipitation intensity. Therefore the VI was designed to detect the precipitation type from the log file. When light precipitations occur, four consecutive recordings are captured. In other cases, only three recordings are captured. The increased number of recordings in light precipitation events is necessary to capture hydrometeors with increased probability.

The maximum number of recordings in a day is 576. The maximum number of recordings is reached, when light precipitations have occurred for the whole day. Since each recording is 20 seconds long, the size of one recording is close to 100 MB. Thus, the maximum amount of data gathered in a day is approximately 58 GB. The recording sequence is started when the main VI meets the trigger conditions. As the conditions are met, the main VI executes a sub VI, which performs the actual recording. The sub VI is presented in Figure 33.

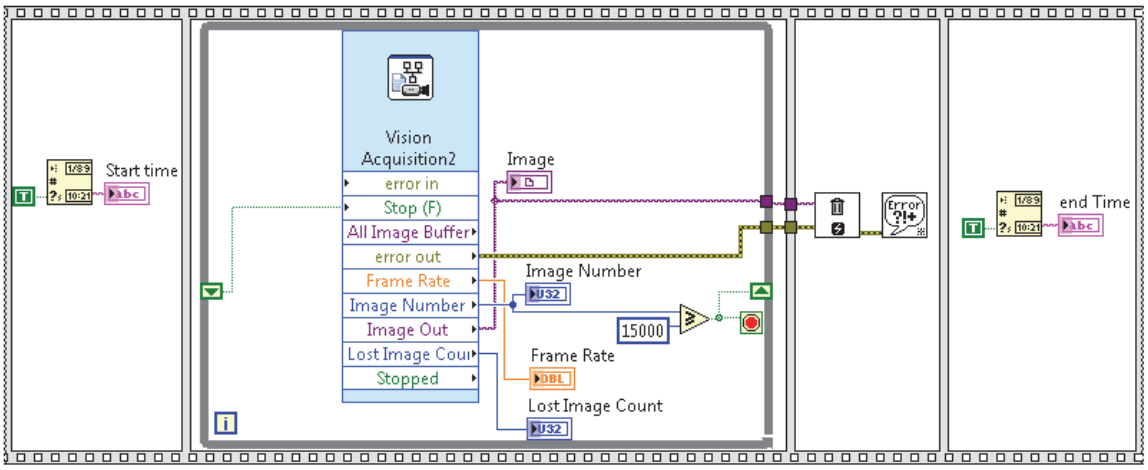

Figure 33. The sub VI of the recording software

As can be seen from Figure 33, the sub VI contains Vision acquisition express VI. The Vision acquisition express VI is utilized to acquire images from the HSC. It has a GUI where acquisition settings of the HSC can be adjusted. The settings could be programmatically set as well. That is beneficial when the settings are required to be changed frequently. As the HSC will record always with the same settings, the programmatic adjustment of the settings is not necessary. The used recording settings are shown in Table 16.

Table 16. The HSC settings.

Settings	
AOI	640 x 480 px
Max frame rate	750 fps
Exposure time	59 µs
Readout mode	Fast

The area of interest (AOI) used for recording is 640 x 480 px. The exposure time is set to 59 us and the readout mode is set to fast, achieving frame rate of 750 fps. The software starts image acquisition immediately when the sub VI is executed. The software continues image acquisition until the acquired image count is 15 000. Since the HSC uses 750 fps, 15 000 images are acquired in 20 seconds. When the required image count is acquired the sub VI saves acquired images as an Audio Video Interleave (AVI) -file and returns to the main VI.

The main VI executes the sub VI three or four times depending on the precipitation intensity. When the target number of recordings is captured, the main VI moves the recording files to the AWORe NAS.

3.3.4 Audio recording software

It was described in Section 3.2.3 that AWORe uses an external microphone for audio recording. The microphone is directly connected to the HSC PC, which runs designed audio recording software. The audio recording software was also developed using LV. The software uses the Acquire sound VI and Sound file write simple VI for audio recording from the microphone input of the secondary PC. The audio recording VI is shown in Figure 34.

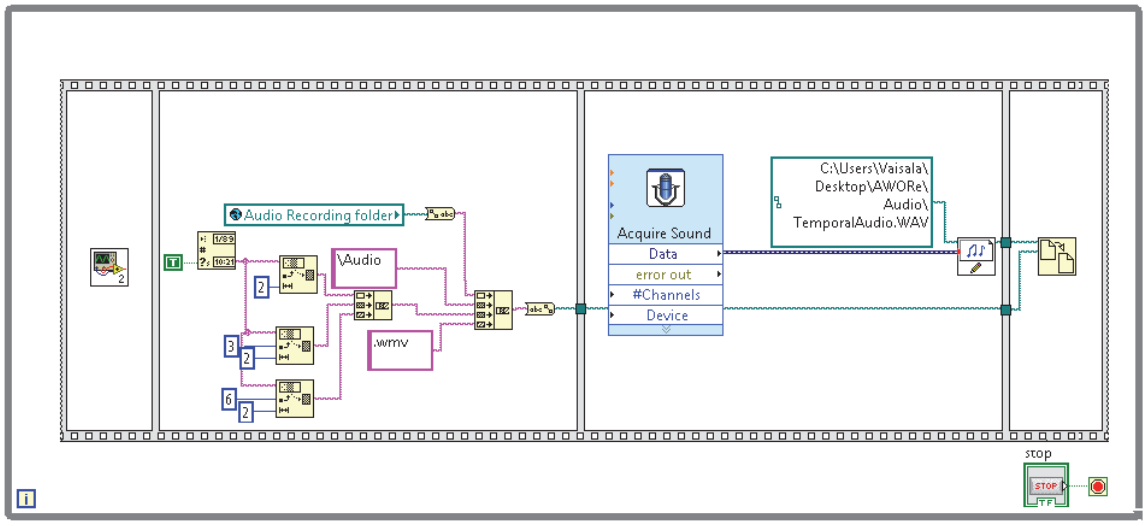

Figure 34. Designed audio recording software

As can be seen from Figure 34, the VI first defines the path where to save the audio file. The recorded audio file is saved to the same folder where the report and HSC recordings are stored. This makes browsing of the files easy for the users. After the path is defined, the VI starts to acquire audio for 300 seconds. When the time has elapsed, the VI writes the acquired sound data to the TemporalAudio.wav file, which is used to temporarily store the audio recording. The temporal file is renamed and moved to the permanent location.

Audio recordings allow observers to listen occurred precipitations. However, this requires observers to listen the recorded audio, demanding resources. In order to automatize audio analysis, spectrum analysis could be utilized in distinguishing between solid and liquid particles. However, in this thesis spectrum analysis of the audio recordings was not in the scope. Since LV has good audio analyzing tools, automatic audio analysis could be implemented to the audio recording software in future.

3.3.5 Web UI

AWORe is required to have a web UI to allow observers to submit observations for AWORe. Human observations are essentially important in observing of infrequent and ambiguous precipitation events, such as hail or mixed precipitations. Observers are able to ensure that AWORe detects events by submitting an observation via the web UI.

The web UI is called Precipitation observation tool and is basically a web page, which is restricted to work only in Vaisala network. The web UI is implemented utilizing HTML5 and PHP 5. The web UI front page is shown in Figure 35.

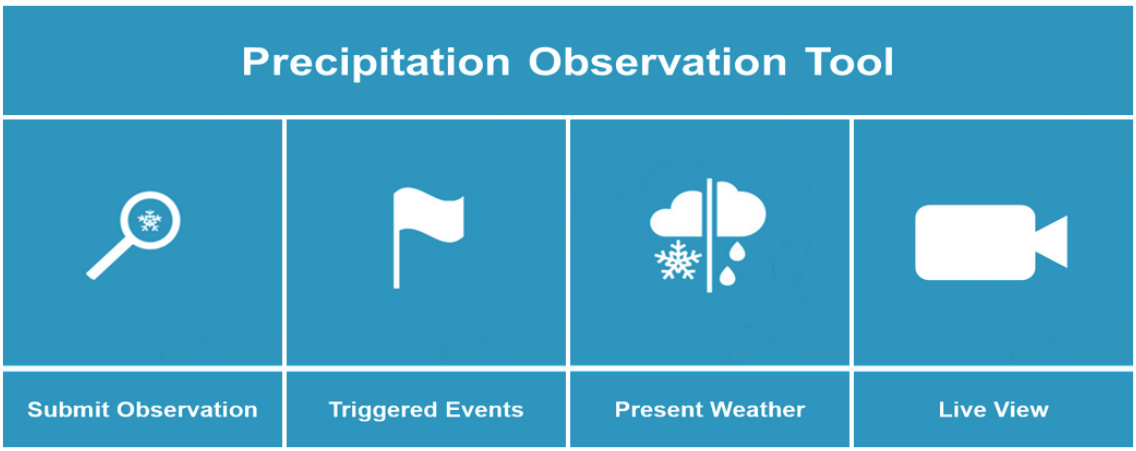

Figure 35. The front page of the web UI

Users may navigate to all pages of the web UI from the front page. The web UI contains the following pages:

- Submit observation
- Triggered events
- Present weather
  - Weather data diagram
  - Triggered events diagram
- Live view

Submit observation page is where users may submit observations. Triggered events page presents all the events triggered during a current day. Present weather page shows real-time weather data and contains links for two distinct diagram pages, which present the weather conditions of the current day. Live view page direct users to live views of network cameras. Submit observation page is presented in Figure 36.

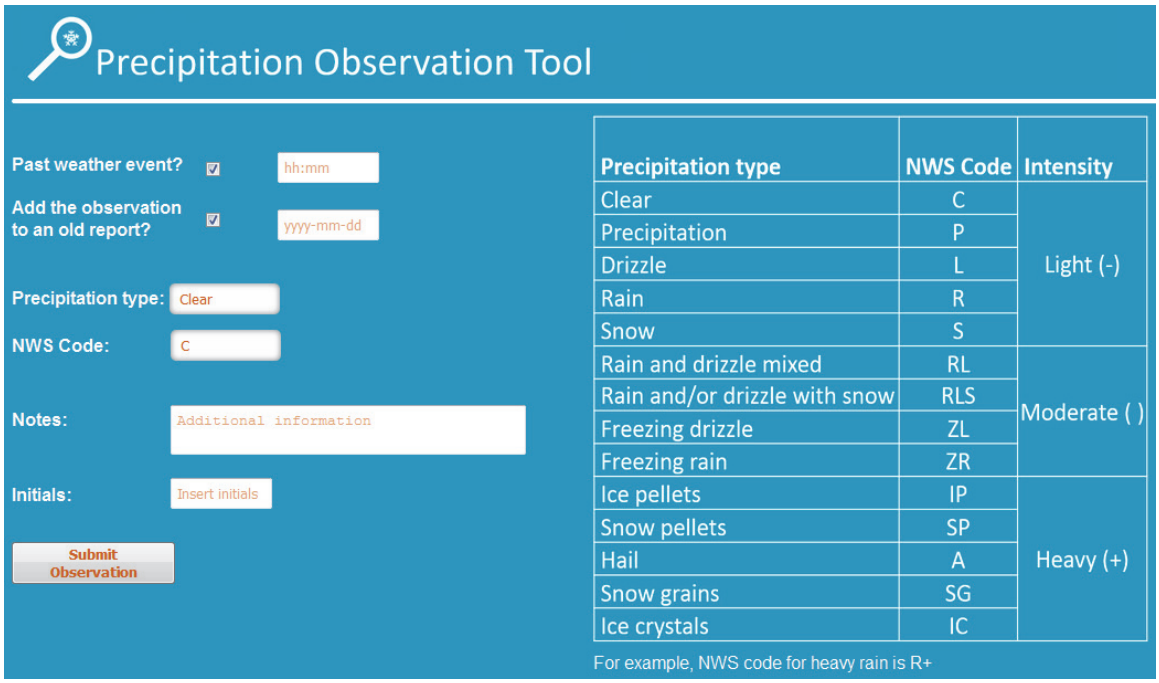

Figure 36. Submit observation page

It can be seen from Figure 36 that the submit observation page contains a form including several fields, which must be filled in order to submit an observation. Observers must define first whether the event is still present or not. If the upper check box is checked, weather event has already passed and the AWORe software does not trigger an event in real-time. In this case, time of the event must be inserted manually to the first text field, when the AWORe software adds the event to the correct position in the report. If the checkbox is unchecked, AWORe triggers an event. The lower check box must be checked if the observed event has occurred during past days. If the check box is checked, observers must define the day when the event was observed so that the AWORe software adds the observation to the report of the correct day.

Next step is to select the observed precipitation type from the upper drop-down menu and corresponding NWS code from the lower drop-down menu below. The table shown in Figure 36 presents all precipitation type and NWS code options included in drop-down menus. The page has also a field for additional information, where the observer may insert any necessary information to clarify the observed event. The observers must insert initials to the last text field so that the observer can be tracked afterwards. The observation is submitted by pressing submit observation button. Submitting an observation adds new line to a user observations log file. The log file contains all user observations of the current day. The AWORe software handles the log file similarly as any other event trigger log file described in Section 3.3.

The submitted data is written to the log file utilizing HTML form action attribute. The action attribute uses POST method in data transfer. The form action attribute is implemented as shown below:

```
<form class="precipitation" id="postValues"
action="values.php" method="post"></form>
```

All the fields on the web page are defined inside the action form. Each field is implemented by using different HTML form elements. The two drop-down menus are implemented utilizing select tag, as shown below:

```
<select class "precipitation" name="precipitationType">
<option>Clear</option>
<option>Precipitation</option>
...
<option>Rain</option>
<option>Drizzle</option>
</select>
```

All three text fields on the page are implemented using text input form elements. The submit observation button is implemented using button tag. The implementation of text input elements and the button tag is presented below:

```
<input name="eventTime" type="text" form="postValues"
style="width: 80px; padding: 5px; color:#D15B05"
placeholder="hh:mm" class="focus"/>

<button type="submit" value="Submit" style="color:
#D15B05; font-weight: bold; width: 150px; ">Submit
Observation</button>
```

As the submit button is pressed, the page transfers data from all fields to values.php file. The page writes the values received via POST method to the user observations log file. Simplified version of the script in values.php file is shown below:

```
$initials = $_POST['initials'];
$precipitationType = $_POST['precipitationType'];
$information = $_POST['information'];
$NWScode = $_POST['NWScode'];
$eventTime = $_POST['eventTime'];
$eventDate = $_POST['eventDate'];

$f = fopen("userObs.txt", "a");
fwrite($f, $dt->format('H:i:s') . "    " . $initials . "
     " . $precipitationType . "     " . $NWScode . "    "
.  $information . "    " . $eventTime . " ". $eventDate
"  ". "\r\n");
fclose($f);
```

It can be seen from the description that a new row containing seven columns is added to the log file every time an observation is submitted. The first column contains automatically generated timestamp. The columns 2-5 contain information about the submitted observation. Last two columns define the time and date of the observation if past event is submitted. Those columns functions also as an indicator for the AWORe software. If the columns are empty, software understands that the submitted weather event is still on-going and event must be triggered. Otherwise, the software only adds the observation to the report of the correct day.

As an observation is submitted, AWORe follows the same procedure as when an event trigger sensor triggers an event. However, observations submitted via the web UI are prioritized, so that the observer initials are always marked to the trigger column in the report (Section 3.3.1). In other cases, the trigger column contains the trigger number that first triggered an event.

Submit observation page contains all features that the web UI is required to have. However, it was found during the AWORe development process that it would be beneficial to be able to follow the events of the current day. Therefore, the triggered events page was designed. The page contains all events triggered during the current day.

The triggered events page contains fundamentally all the same information as the daily-generated report presented in Section 3.3.1. Basically, the only difference is that the page contains a direct link to the video recording related to the triggered event, in the camera recording columns that directly open the camera recordings, whereas the report contains the actual file path. The page shows all acquired weather parameters at the time of triggered events.

Additionally, Present weather page was designed, allowing real-time monitoring of occurring weather conditions. The page shown latest values from all sensors. The page also includes date and time of the latest observation. Present weather page is presented in Figure 37.

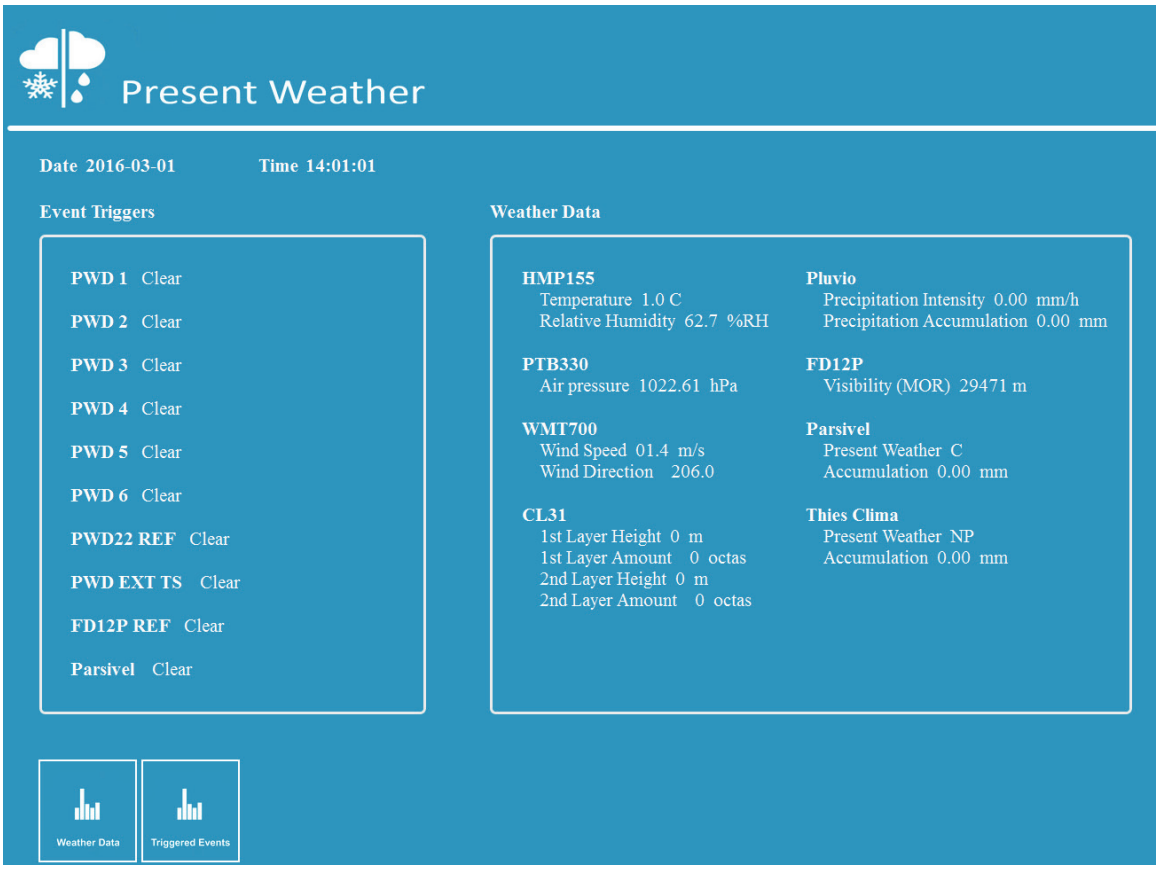

Figure 37. Present weather page

The AWORe software writes the latest values to the HTML-file every 30 seconds. Thus, the values are updated to the page every 30 seconds. In addition to the present weather view, the page contains two buttons that direct user to diagrams, which present the occurred weather of the day. The first diagram page presents weather data in three diagrams. The second diagram page presents triggered events in one diagram, allowing users to easily see states of each event trigger sensor.

The diagrams are implemented utilizing Chart.js open source HTML5 chart. Chart.js includes several different chart types from which only line chart is used on the web page. Chart.js contains a template for the line chart, which must be modified using JavaScript to achieve adequate diagrams for the web UI. On the first diagram page, the first diagram presents basic weather data. The second diagram presents visibility and cloud data on logarithmic scale. The third diagram presents precipitation accumulation on logarithmic scale. The first diagram is presented in Figure 38. [56]

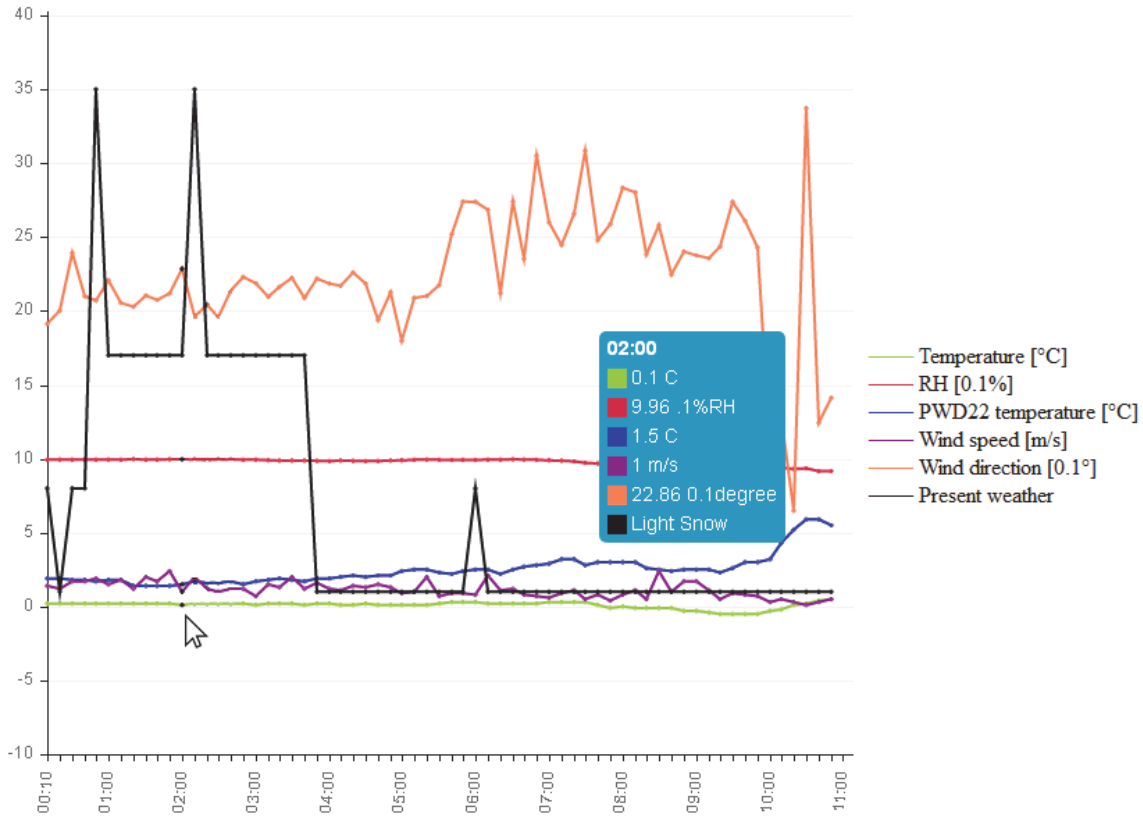

Figure 38. Weather data diagram

As can be seen from Figure 38, the diagram contains six datasets. Each dataset is styled by adjusting different styling parameters, such as stroke color. In addition to the styling parameters, each dataset has individual label. The label is set to be same as the unit of the dataset. Only exception in the labels is the label of PWD22, whose label is set to "PW". The units are used as labels to distinguish between the datasets and also to easily see the units in the chart tooltip shown in Figure 38. The tooltip is used to ease examination of single points on the diagram. The tooltip is modified by modifying multiTooltipTemplate setting. The tooltip of the weather data diagram contains values and units at a point pointed with the cursor (Figure 38).

The values are presented as float numbers except present weather value reported by PWD22. The present weather value is presented as precipitation type. In order to present precipitation type in the tooltip as in Figure 38, multiTooltipTemplate setting must be modified. The following function was designed and added to the multiTooltipTemplate setting to achieve the presented tooltip:

```
multiTooltipTemplate: function(datasetLabel){
   switch(datasetLabel.datasetLabel){
                case "PW":
                return  datasetLabel.value.toString()
                 .replace("40", "Heavy Hails")
                 .replace("39", "Hail")
                 .replace("38", "Light Hail")
                 ...
                 .replace("2","Light Precipitation")
                 .replace("1","Clear")
                 .replace("0", "N/A");
                break;
                default:
                return  datasetLabel.value.toString();
    }
 }
```

The function described above contains a switch statement, which has a case for datasets labeled as “PW” and a default case. The switch statement determines whether a parameter must be presented as a precipitation type or not. Each precipitation type is converted to a numeric value by AWORe software. The numeric values and corresponding precipitation types are shown in Table 17.

Table 17. The numeric expression of precipitation types.

No.	Precipitation type
0	N/A
1	Clear
2-4	Precipitation
5-7	Drizzle
8-10	Rain
11-13	Rain and drizzle
14-16	Rain and/or drizzle and snow
17-19	Snow
20-22	Snow pellets
23-25	Snow grains
26-28	Freezing drizzle
29-31	Freezing rain
32-34	Ice crystals
35-37	Ice pellets
38-40	Hail

It can be seen from Table 17 that each precipitation type has three values. The lowest value of the range always presents light intensity, whereas the highest number presents heavy intensity.

The numeric values are written to global variables simultaneously as the NWS code is transformed to actual precipitation type strings by the AWORe software. As shown in the script description, the function returns a string where the numeric value is replaced by the defined string. If the label is unequal to “PW”, the function only returns the original dataset value. This method is used in multiTooltipTemplate if the tooltip contains present weather and numeric values mixed.

As described earlier in this section, the two other diagrams on the first diagram page use logarithmic scale to enhance examination of the values. The visibility and cloud data diagram is shown in Figure 39.

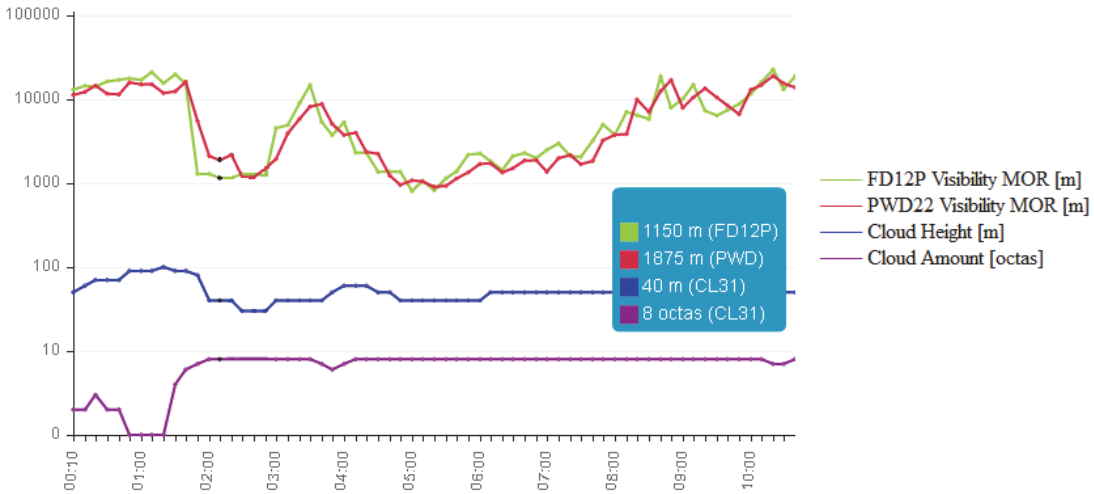

Figure 39. Visibility and cloud data diagram

The Chart.js does not natively have logarithmic scale. Thus, implementation of the logarithmic scale was designed in this thesis. First, the scale of the diagram was modified using the designed function:

```
scaleLabel: function(label){
     switch(label.value){
     case "1":
     return label.value.toString().replace("1", "10");
     break;
     case "2":
     return label.value.toString().replace("2", "100");
     break;
     ...
     case "5":
     return label.value.toString().replace("5","100000");
     break;
     default:
     return label.value.toString().replace("0", "0");
```

The dataset values are converted to 10-base logarithm by the AWORe software as the software writes the chart-file. The chart draws the data points correctly and the logarithmic values are re-converted for the tooltip, modifying the multiTooltipTemplate as follows:

```
multiTooltipTemplate: function(datasetLabel){
            switch(datasetLabel.value){
            case 0:
            return datasetLabel.value.toString()+ ' ' +
                   datasetLabel.datasetLabel;
            break;
            default:
            return Math.pow(10, datasetLabel.value,2).
                   toFixed(0) + ' ' +
                   datasetLabel.datasetLabel;
```

The described functions are used in both logarithmic scales with the difference that in the diagram that presents precipitation accumulation, the logarithmic scale is from 0 to 100.

The second diagram page presents the reported condition of each event trigger sensor at each point. The diagram is presented in Figure 40.

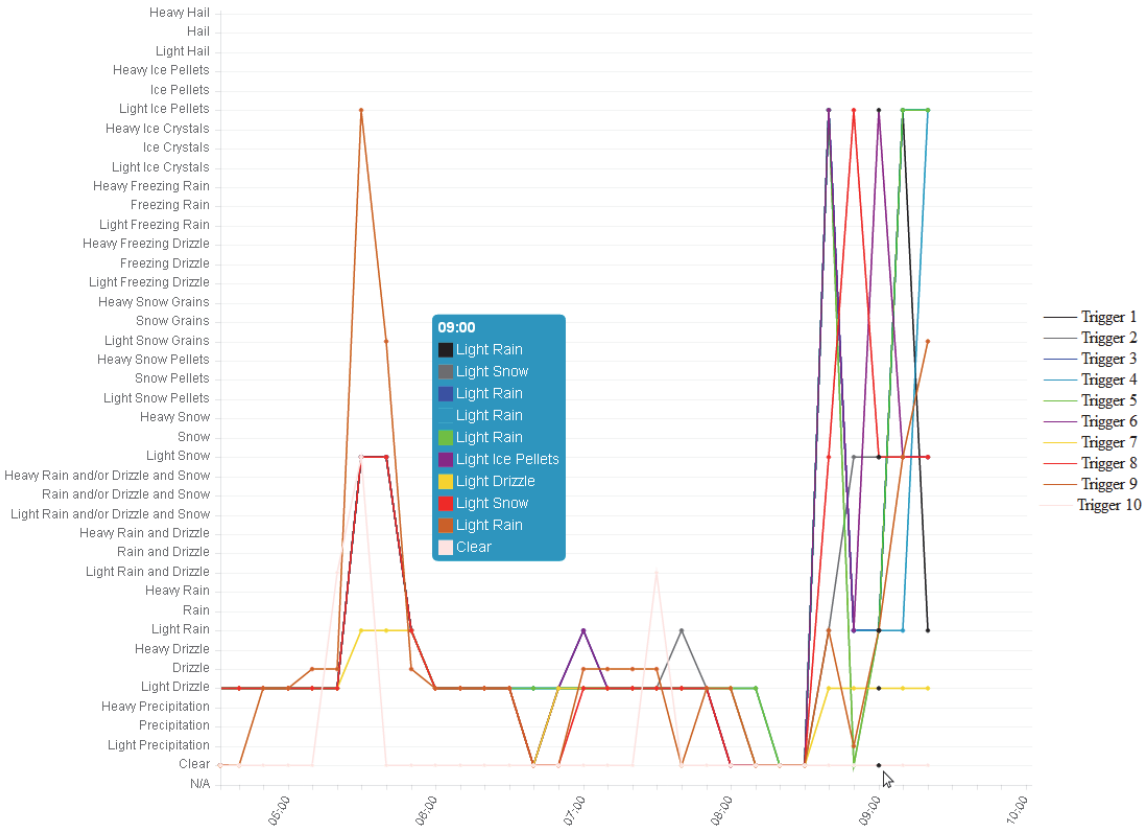

Figure 40. Diagram presenting event trigger sensor reports

As can be seen from Figure 40, the event trigger sensors can be easily compared using the diagram. However, the diagram has resolution of 10 minutes and does not indicate all changes in the states of the sensors. Consequently, performing comprehensive intercomparison between the event trigger sensors requires utilization of the daily generated report or the log file. Nevertheless, the diagram provides good general view of the events detected during the day.

The live view page contains direct links for both network camera streams. The live view page is shown in Figure 41.

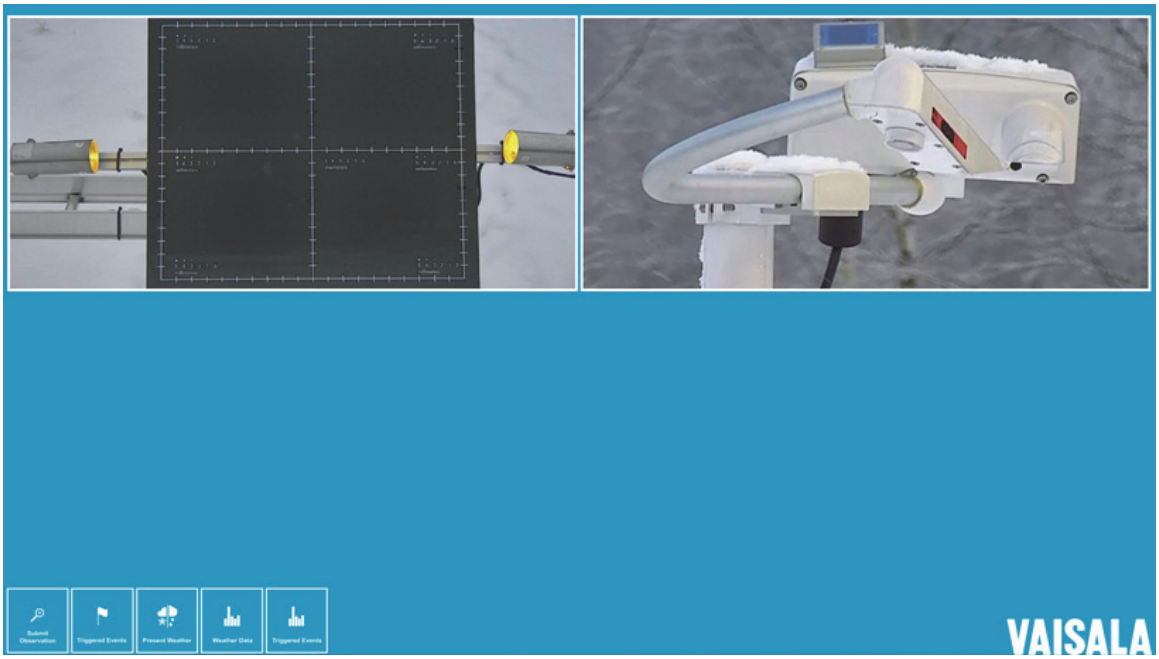

Figure 41. The live view page

The users are able to open the live streams by pressing the camera views on the page (Figure 41). Since the web UI has all the features described in this section, the web UI allows observers to submit observations as well as to easily monitor real-time and past weather conditions utilizing the various pages of the web UI.

4 AWORe evaluation

In this chapter, the implementation of AWORe is evaluated. Section 4.1 evaluates used audio and video recording methods. Section 4.2 discusses the applicability of AWORe for PWS evaluation.

4.1 Evaluation of audio and video recording methods

AWORe was required to allow human observers to determine the precipitation occurring at any given time without requiring human observers to be continuously present. This demands opportunity to visually examine occurring precipitations and assistance of weather data. In addition, observers must be able to determine the terminal velocity, size and state of hydrometeors, to achieve more reliable results.

Since no trained observers were available during the evaluation period, the applicability of AWORe for precipitation type classification was unable to be evaluated in this thesis. Consequently, this section only evaluates the applicability of AWORe recordings for visually detecting the occurrence of precipitations as well as determining the terminal velocity, size and state of hydrometeors.

AWORe records both video using two network cameras and a HSC, as well as audio using a microphone. As presented in Chapter 3, network cameras were designed to continuously record a general view of the current precipitation, allowing the type and character of precipitation to be identified visually. Primary camera recordings are essentially used to determine the precipitation type and character as well as to estimate hydrometeor size and terminal velocity, whereas the secondary camera is primarily used to detect any accumulation of ice and snow on event trigger sensors. The HSC is recording only during precipitation events and the recordings are used for closer examination of hydrometeors. For example, the terminal velocity and size of hydrometeors can be more precisely determined from HSC recordings.

Captured network camera recordings indicate that the occurrence of precipitations is well detectable. The primary camera recordings showed that even light precipitation events are well detectable, due to the contrast plate. Secondary camera recordings showed that any snow, ice or water accumulation on event trigger sensors is well detectable at daytime, as shown in Figure 42.

Figure 42. Secondary camera view of Vaisala PWD52 at day and night

It can be seen from Figure 42 that in dark conditions the accumulation is more challenging to detect. Estimation of hydrometeor terminal velocity and size assists in determining the precipitation type when precipitation type cannot be visually identified precisely. The primary camera recordings allow observers to make only rough estimations of the measures, due to its relatively long exposure time and low frame rate. An example image captured from primary camera recording during a heavy snow event reported by the most of the event trigger sensors is presented in Figure 43.

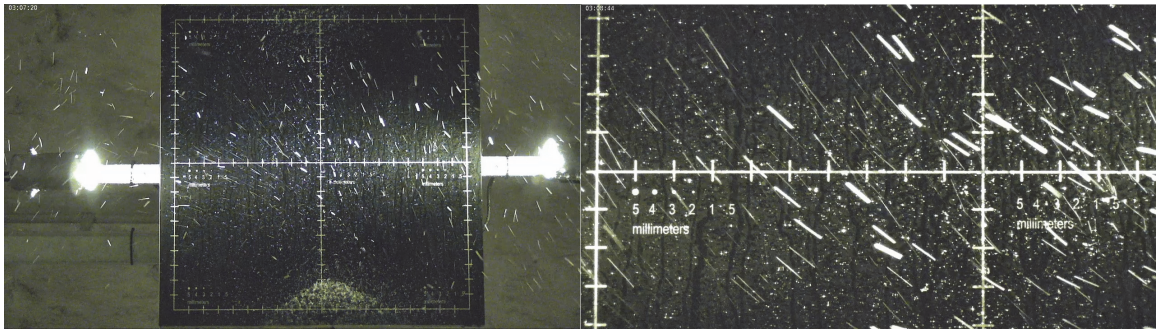

Figure 43. Primary camera view during a heavy snow event

It can be seen from Figure 43 that snowflakes are appearing as stripes in the still image, indicating that network cameras are unable to clearly capture individual hydrometeors, due to insufficient exposure time, as described earlier in Section 3.2.1. Nevertheless, Figure 43 shows that the size of snowflakes can be well estimated by measuring the width of the stripes. The same applies for other hydrometeor types as well. Estimating the terminal velocity from the primary camera recordings is more challenging and cannot be done precisely. The length of the stripes could be used for determination of the terminal velocity, if the exposure time would be manually adjusted. However, automatic exposure time adjustment is used to ensure optimal brightness in recordings.

In order to reliably identify the precipitation type, the state of a hydrometeor must be determined, in addition to the terminal velocity and size estimation. However, distinguishing between frozen and liquid hydrometeors is challenging, since they both may be transparent.

For example, ice pellets can be difficult to distinguish from rain in primary camera recordings, whereas snow is easier to recognize, due to the color and shape of snowflakes. Nevertheless, the collector plate displayed in secondary camera recordings assist in distinguishing between liquid and solid hydrometeors as solid particles bounces when they hit the surface and also remain on the collector plate, whereas liquid hydrometeors flow away from the plate. The collector plate view during a suspected snow pellet event is shown in Figure 44.

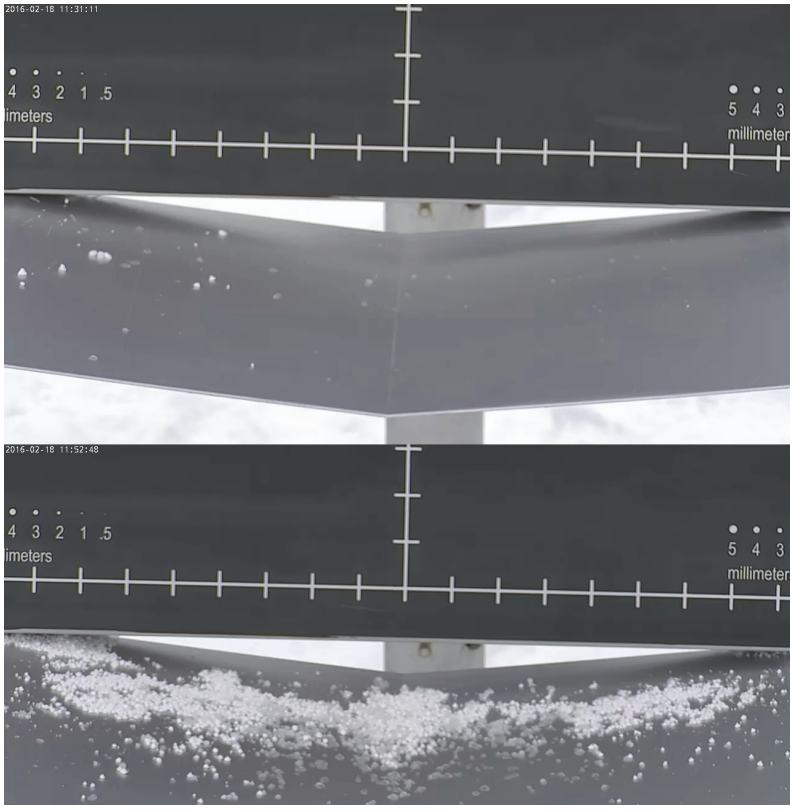

Figure 44. Collector plate view during a suspected snow pellet event

As can be seen from Figure 44, solid hydrometeors remain on the collector plate. The author noted during the same event that audio recordings assist in differentiating between solid and liquid particles.

HSC recordings are utilized for more precise examination of hydrometeors. The terminal velocity, size and state of hydrometeors can be well determined, since the HSC is able to capture at least two images of hydrometeors falling through its FOV (Section 3.2.2).

The contrast plate used with the HSC has a grid printed on its surface (Figure 21), allowing precise estimation of the terminal velocity. Additionally, the dots on the contrast plate enable precise estimation of the size. Two frames captured by the HSC during a light snow event are shown in Figure 45.

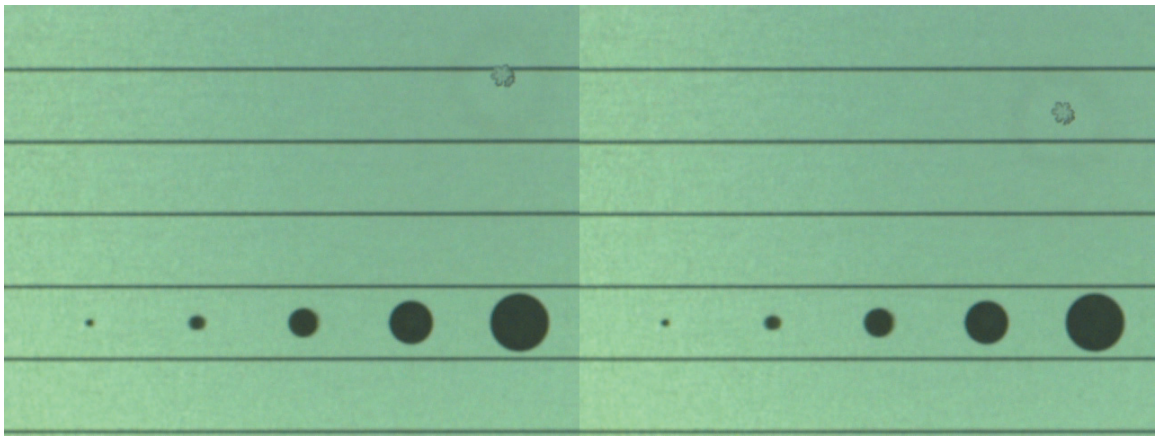

Figure 45. Two frames captured by the HSC during light snow event

The hydrometeor size was estimated to be 1.8 mm by comparing the hydrometeor to the dots on the background (Figure 45). It can be seen from Figure 45 that the hydrometeor falls approximately 2.5 mm between two frames. Since the time between two frames is 1.33 ms when the frame rate of 750 fps is used, the terminal velocity can be precisely determined. Using Equation 15, the terminal velocity was calculated to be 1.9 m/s. The fastest hydrometeor during the evaluation period was captured during a suspected ice pellet event and is shown in Figure 46.

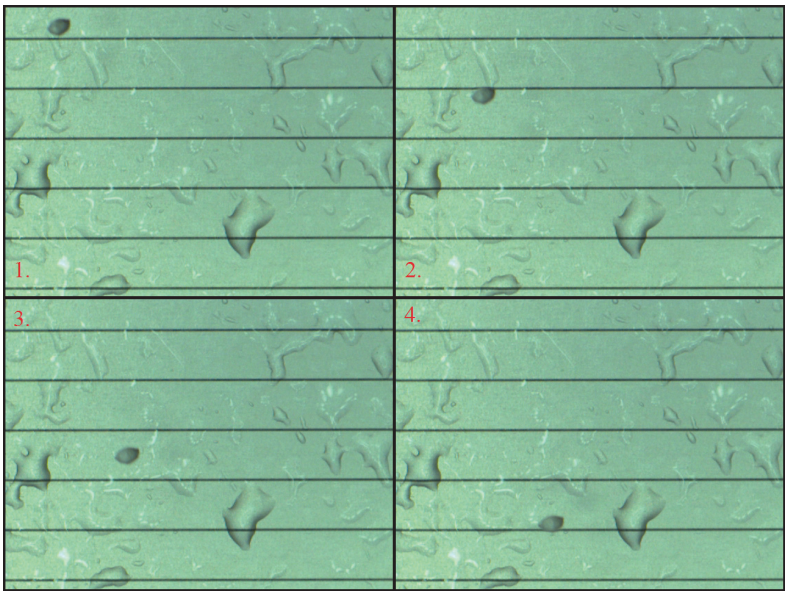

Figure 46. The HSC recording during a suspected light ice pellet event

It can be seen from Figure 46 that the hydrometeor is not spherical and its shape does not change, indicating that the hydrometeor is frozen. The moved distance of the hydrometeor between two frames is estimated to be 7.5 mm. The terminal velocity was calculated to be 5.6 m/s using Equation 15. Although the dots on the contrast plate are not visible in Figure 46, the size of the hydrometeor can be estimated, since the space between the horizontal lines is known to be 5 mm (Figure 21). The size of the hydrometeor is estimated to be 2 mm.

Since the highest terminal velocity measured during the evaluation period was 5.6 m/s, the applicability of the HSC to capture faster hydrometeors was unable to verify. Nevertheless, the results presented in this section endorse the calculations presented in Section 3.2.2. Thus, it can be assumed that the HSC is able to clearly capture hydrometeors with terminal velocity of 8.5 m/s. Hydrometeors that may reach such a terminal velocity are, e.g., rain droplets larger than 4 mm and hail larger than 5 mm (Figure 5). However, AWORe is required to capture hydrometeors with terminal velocity of 10 m/s. Thus, the HSC does not completely fulfill the requirements.

Since not all precipitation types occurred during the evaluation period, it can only be assumed that rain and drizzle in their freezing state would be difficult to observe from recordings, since they resemble rain and drizzle as they fall. Moreover, the sounds generated by freezing rain and drizzle probably resemble that generated by rain and drizzle, when the state of hydrometeors cannot be determined reliably from audio recordings. Nevertheless, freezing precipitations can be most likely detected from secondary camera recordings if significant ice accumulation occurs on the event trigger sensors or on the collector plate.

The results presented in this section indicate that the implemented audio and video recording methods are sufficient in order to determine the terminal velocity, size and state of hydrometeors as well as to visually examine the appearance of hydrometeors. Since the applicability of AWORe for precipitation type classification was not verified in this thesis, it can only be assumed that most of the precipitation types can be classified using AWORe.

4.2 Applicability of AWORe for PWS evaluation

The purpose of AWORe is to allow human observers to determine the precipitation occurring at any given time without requiring human observers to be continuously present. The human observations are required for performance evaluation of PWSs, which is the main use of AWORe. Evaluation methods of PWSs were introduced in Section 2.2.2.

It was described that basically two different evaluation methods are used and the intercomparison between human observer and PWS is the only reliable evaluation method. Nevertheless, intercomparison between PWSs is necessary when the consistency of PWSs is investigated.

AWORe was designed to utilize 10 event trigger sensors that detect changes in present weather. An event is triggered every time any of the event trigger sensors detects a change in present weather. Triggered events are written to the daily report. In addition, the daily log file contains all measurement results with 1 minute time difference. Thus, AWORe can be used for intercomparison between PWSs without requiring any actions from observers during the evaluation period. Observers or other professionals are only needed to analyze the data. Furthermore, observers are able to submit observations and monitor occurring conditions via the web UI. The event trigger sensors can be changed whenever necessary, allowing intercomparison of different types of PWSs.

The same data used in intercomparison between PWSs can be used in intercomparison between human observer and PWSs as well. However, human observers are required to determine the occurred conditions using AWORe recordings. As presented in Section 4.1, occurred precipitations can be detected and it was assumed that the precipitation types can be identified using AWORe recordings. Observers are required to determine the weather conditions for the whole evaluation period by analyzing the recordings. Although relatively much resource is required to determine the weather conditions from the recordings, the human observers are not required to be present during the evaluation period. In addition, observers may primarily focus on the triggered events. However, in order to determine the verification scores, missed events must be searched from the recordings as well. Nevertheless, records can be played with higher playback speed, decreasing the time required for viewing the recordings.

AWORe also allows observers to analyze gathered data as a group, thus enabling the likelihood of more precise results. This is beneficial due to the subjectivity of human observations (Section 2.2.2). Overall, AWORe allows performance evaluation of PWSs using both evaluation methods with less resource than those currently required, fulfilling its purpose very well.

5 Conclusions

In this thesis, precipitation and currently used automatic precipitation observation methods were introduced. In addition, the development process of AWORe was described. The goal of this thesis was to develop and implement AWORe for continuously recording weather conditions occurring at the Vaisala test field. AWORe was designed to utilize two network cameras, a microphone, a HSC and numerous weather instruments. The AWORe software was designed to connect all individual parts of AWORe to form a system. Additionally, the audio recording software and the HSC software were developed. Furthermore, the web UI was designed, allowing users to submit weather observations as well as to monitor real-time and past weather conditions.

Various requirements were defined for AWORe, which were considered in AWORe development. AWORe was successfully implemented and was found during the evaluation period to function as designed. AWORe contains all the required components and the HSC is the only component that does not completely fulfill the requirements. The HSC was required to capture hydrometeors that have terminal velocity of 10 m/s with motion blur of 0.5 mm. However, the HSC was estimated to be unable to capture hydrometeors faster than 8.5 m/s with the motion blur of 0.5 mm, due to the insufficient shutter speed.

The fastest hydrometeor detected during the AWORe evaluation period had terminal velocity of 5.6 m/s. Consequently, it can only be assumed that the HSC is able to capture hydrometeors with terminal velocity of 8.5 m/s relying to the calculations. Nevertheless, occurrence of hydrometeors with such a terminal velocity is quite infrequent in Finland, allowing the HSC to clearly capture most of the hydrometeors. By analyzing all audio and video recordings, observers are able to determine the terminal velocity, size and state of hydrometeors. It was also assumed in this thesis that most of the precipitation types can be classified using AWORe.

AWORe was verified to be applicable for performance evaluation of PWSs using both of the two evaluation methods introduced in this thesis. The daily-generated report indicates the precipitation events occurred during the day and provides comprehensive weather data, which is beneficial for classification of precipitation types. The web UI allows observers to submit precipitation observations and the diagrams on the web UI enable easy examination of the current weather conditions. Additionally, the triggered events page provides information of the triggered events during the day before the report is generated. Thus, the users may easily follow the weather conditions during a day.

In future, the HSC could be replaced by a HSC that has faster shutter speed and higher frame rate. Since the HSC software utilizes USB3 Vision interface, the HSC can be easily replaced by another HSC supporting the interface. In addition, future research could investigate solutions for automatic hydrometeor detection from the HSC recordings to decrease the time required for viewing the recordings. Since LV has good signal processing tools, possibilities for automatic detection of liquid and frozen precipitations from audio recordings could be investigated as well.

The detectability of freezing precipitations was assumed to be difficult from current recordings. Consequently, methods for better detectability of freezing precipitations should be developed in future. For example, soundings data could be used for detection of the vertical profile typically occurring during freezing precipitations.

References

[1] Hanna-Leena Merenti-Välimäki, Jan Lönnqvist and Pertti Laininen, “Present weather: comparing human observations and one type of automated sensor”, *Meteorological Applications*, vol. 8, no. 4, pp. 491-492, Dec. 2006.

[2] BASIC COMMERCE AND INDUSTRIES INC. and Volpe National Transportation Systems Center, “Weather Observation Improvements (WOI) Winter Weather Concept Maturity Level 4 CMTD Demonstration Plan: 2015-2016 Update”, 2015.

[3] H. Karttunen, J. Koistinen, E. Saltikoff and O. Manner, "Ilmakehä ja sää", *Ursa*, pp. 40, 151-152, 190- 201, ISBN 222-225. 952-5329-17-8, 2001.

[4] Henry G. Houghton, "Cloud Physics", *Science*, vol. 129, no. 3345 , pp. 311-312, Feb.1959.

[5] Lynn E. Newman, "Moisture, Stability and Precipitation", http://web.gccaz.edu/~lnewman/gph111/topic_units/moisture/moisture_stabil_prec/moisture_stabil_prec2.html. Accessed 14.01.2016.

[6] Gerard H. Roe, "Orogprahic Precipitation", *Annual Review of Earth and Planetary Sciences*, vol. 33, pp. 656-658, May. 2005.

[7] Ryan J. Zerr, "Freezing Rain: An Observational and Theoretical Study", *Journal of Applied Meteorology*, vol. 36, no. 12, pp. 1647-1648, 1997.

[8] Critical Zone Observatory, "Code Table SYNOP/METAR". http://www.czo.psu.edu/downloads/Metadataworksheets/LPM_SYNOP_METAR_key.pdf. Accessed 14.10.2015.

[9] WMO, “Guide to Meteorological Instruments and Methods of Observation”, WMO-No. 8, pp. I.6-1-2, I.6-8-10, I.9-10-11, I.14-3-4, II.2-9-10, 2008.

[10] Paul T. Willis, "Functional Fits to Some Observed Drop Size Distributions and Parameterization of Rain", *Journal of the Atmospheric Sciences*, vol. 41, no. 9, pp. 1650- 1651, May. 1984.

[11] Robert M. Rauber and Ali Tokay, "An explanation for the Existence of Supercooled Water at the Top of Cold Clouds", *Journal of the Atmospheric Sciences*, vol. 48, no. 8, p. 1020, Apr. 1991.

[12] FMI, "Ilmastokatsaus", ISSN: 1239-0291, pp. 4-5, Feb. 2006.

[13] FAA, "In-Flight Icing Operations and Training Recommendations", https://www.faa.gov/other_visit/aviation_industry/airline_operators/airline_safety/safo/all_safos/media/2010/SAFO10006.pdf. Accessed 4.2.2016.

[14] NWS, “Precipitation types”, http://www.srh.noaa.gov/srh/jetstream/global/preciptypes.htm. Accessed 5.1.2016.

[15] ICAO, "Manual of Runway Visual Range Observing and Reporting Practices", pp. 4-4, 2012.

[16] Ross Gunn and Gilbert D. Kinzer, “The Terminal Velocity of Fall for Water Droplets in Stagnant Air August”, *Journal of Meteorology*, vol. 6, pp. 243-248, 1949.

[17] R. A. Ellis, A. P. Sandford, G. E. Jones, J. Richards, J- Petzing and J. M. Coupland, “New laser technology to determine present weather parameters”, *Measurement Science and Technology*, vol 17, no. 7 pp. 1715-1722, Jun. 2006.

[18] NASA, “Terminal Velocity”, http://www.grc.nasa.gov/WWW/K-12/airplane/termv.html. Accessed 8.2.2016.

[19] A. F. Spilhaus, “Raindrop Size, Shape, and Falling Speed”, *Journal of Meteorology*, vol. 5, no. 3, pp. 108-109, Jun. 1948.

[20] Jussi Leinonen, Dmitri Moisseev, Matti Leskinen and Walter A. Petersen, “A Climatology of Disdrometer Measurements of Rainfall in Finland over Five Years with Implications for Global Radar Observations”, *Journal of Applied Meteorology and Climatology*, vol. 51, no. 2, p. 396, Feb. 2012.

[21] IVAO, “How to Decode METAR, TAF, and Pilot Reports”, https://www.ivao.aero/training/tutorials/metar/metar.htm. Accessed 27.10.2015.

[22] Jitze P. van der Meulen, “Exploratory actions on automatic present weather observations”, *EUMETNET*, pp. 3-4, 17-21, 2003.

[23] WMO, “Guide To Climatological Practices – Third Edition”, p. 22, 2009.

[24] OTT Hydromet, “OTT Pluvio² - Weighing Rain Gauge”, http://www.ott.com/en- us/ products/meteorological-sensors/ott-pluvio2-8/. Accessed 2.11.2015.

[25] Campbell Scientific, “PWS100 Present Weather Sensor”, http://campbellsci.eu/pws100. Accessed 17.11.2015.

[26] Vaisala Oyj, ”Vaisala Present Weather Detectors PWD22 and PWD52”, http://www.vaisala.com/en/products/presentweathersensors/Pages/PWD2252.aspx. Accessed 17.11.2015.

[27] Belfort Instrument, “Present Weather Sensor Model 6550”, http://belfortinstrument.com/products/present-weather-sensor-model-6550/. Accessed 17.11.2015.

[28] Biral, “VPF-710 Visibility Sensor”, http://www.biral.com/product/vpf-710-visibility-sensor/. Accessed 17.11.2015.

[29] FAA, “Automated Surface Observing System User's Guide”, pp. 34-36, 1998.

[30] FAA, “United States Experience Using Forward Scattermeters for Runway Visual Range”, pp. 6-7, 25, 1997.

[31] K. Okuyama, ”Laser Light Scattering”, http://aerosols.wustl.edu/AAARworkshop08/ materials/Okuyama/Sub2/2-2.htm. Accessed 28.1.2016.

[32] WMO, “Observing Systems Capability Analysis and Reviews”, http://www.wmo-sat.info/oscar/variables/view/209. Accessed 28.10.2015.

[33] FAA, “Performance Specification PC Based Runway Visual Range (RVR) systems”, p. 38, 2006.

[34] Vaisala Oyj, “Vaisala Visibility Sensor PWD10/20/50 User's Guide”, pp. 17-18, 2013.

[35] Ralph G. Eldridge, “a Few Fog Drop-Size Distributions”, *Journal of Meteorology*, vol. 18, p. 673. Oct. 1961.

[36] KNMI, “Automated discrimination of precipitation type using the FD12P present weather sensor: evaluation and opportunities”, http://citeseerx.ist.psu.edu/viewdoc/download?doi =10.1.1.155.46&rep=rep1&type=pdf. Accessed 24.2.2016.

[37] Joseph T. Schaefer, “The Critical Success Index as an Indicator of Warning Skill”, *Weather and Forecasting”*, vol. 5, p. 571, Jul. 1990.

[38] Kinovea, “Basic High-Speed Video Camera Considerations & Cameras”, http://www.kinovea.org/en/forum/viewtopic.php?id=435. Accessed 3.2.2016.

[39] Sidney F. Ray, “Scientific Photography and Applied Imaging”, pp. 47, 105-106, ISBN 13: 978-0-240-51323-2. 1999.

[40] Warren J. Smith, “Modern Optical Engineering- Third Edition“, p. 152, ISBN 0-07-136360-2, 2000.

[41] Ralph E. Jacobson, Sidney F. Ray, Geoffrey G. Attridge, Norman R. Axford, “The Manual of Photography: Photographic and Digital Imaging - Ninth Edition”. p. 65, ISBN-13: 978-0-240-515748, 2000.

[42] Fujifilm, “Fujinon CCTV Lens for FA/Machine Vision”.http://media.oem.se/Archive /FilesArchive/103182.pdf. Accessed. 3.2.2016.

[43] T. J. Garrett, C. Fallgatter, K. Shkurko, and D. Howlett., “Fall speed measurement and high-resolution multi-angle photography of hydrometeors in free fall”, *Atmospheric Measurement Techniques*, vol. 5, p. 2626, 2012.

[44] Idaku Ishii, Tetsuro Tatebe, Qingyi Gu, Yuta Moriue, Takeshi Takaki and Kenji Tajima “2000 fps Real-time Vision System with High-frame-rate Video Recording”, *IEEE International Conference on Robotics and Automation*, p. 1536, May 2010.

[45] AXIS Communications, “AXIS Q60-E PTZ Dome Network Cameras”, http://www.axis.com/files/datasheet/ds_q60e_60196_en_1411_lo.pdf. Accessed 12.10.2015.

[46] AXIS Communications, “Installation Guide AXIS T8351 Midspan 60W”, http://www.axis.com/files/manuals/ig_t8134_60125_en_1411.pdf. Accessed. 12.10.2015.

[47] AXIS Communications, “AXIS T83 Microphones”, http://www.axis.com/files/datasheet/ds_t83_54493_en_1401_hi.pdf. Accessed 12.10.2016.

[48] Vaisala Oyj, “HMP155 Humidity and Temperature Probe”, http://www.vaisala.com/Vaisala%20Documents/Brochures%20and%20Datasheets/HMP155-Datasheet-B210752EN-E-LoRes.pdf. Accessed 30.10.2015.

[49] Vaisala Oyj, “Vaisala HUMICAP Sensor for Measuring Relative Humidity”, http://www.vaisala.com/Vaisala%20Documents/Technology%20Descriptions/HUMICAPTechnology-description-B210781EN-C.pdf. Accessed 30.10.2015.

[50] Vaisala Oyj, “PTB330 Digital Barometer for Professional Meteorology, Aviation, and IndustrialUsers”,http://www.vaisala.com/Vaisala%20Documents/Brochures%20and%20Datasheets/PTB330-datasheet-B210708EN-E.pdf, Accessed 30.10.2015.

[51] Vaisala Oyj, ”Vaisala Ceilometer CL31 User's Guide”, pp. 49-52, 2015.

[52] Vaisala Oyj, “Weather Sensor FD12P User's Guide”, ss. 21-22, 2002.

[53] OTT Hydromet, “OTT Pluvio² - Weighing Rain Gauge”,http://www.ott.com/en-us/products/meteorological-sensors/ott-pluvio2-weighing-rain-gauge/. Accessed 10.12.2015.

[54] OTT Hydromet, “OTT Parsivel- Enhanced precipitation identifier and new generation of present weather sensor by OTT Messtechnick”, http://www.ott.com/download/ott-parsivel-white-paper/. Accessed 10.12.2015.

[55] Peter M. Chen, Edward K. Lee, Garth A. Gibson, Randy H. Katz and David A. Patterson, “RAID: High-performance, reliable secondary storage”, *ACM Computing Surveys*, vol. 25, pp. 154-157, Jun. 1994.

[56] Nick Drownie, “Chart.js.”, http://www.chartjs.org/, Accessed 7.1.2016.